Hydrol. Earth Syst. Sci. Discuss., doi:10.5194/hess-2016-272, 2016
Manuscript under review for journal Hydrol. Earth Syst. Sci.
Published: 16 June 2016

Hydrology and Earth System Sciences
Discussions

Bridging glacier and river catchment scales: an efficient representation of glacier dynamics in a hydrological model

Michel Wortmann[1,2], Tobias Bolch[3,4], Valentina Krysanova[1], and Su Buda[5]

[1]Potsdam Institute for Climate Impact Research, Telegraphenberg A31, 14473 Potsdam, Germany
[2]Department of Geography, University College London, Gower Street, London WC1E 6BT, United Kingdom
[3]Department of Geography, University of Zurich, Winterthurer Strasse 190, 8057 Zuerich, Switzerland
[4]Institute for Cartography, Technische Universität Dresden, 01069 Dresden, Germany
[5]National Climate Centre, Chinese Meteorological Administration, No. 46, Zhongguancun South Street, Beijing, China

Correspondence to: Michel Wortmann (wortmann@pik-potsdam.de)

Abstract. Glacierised river catchments have been shown to be highly sensitive to climate change, while large populations depend on the water resources originating from them. Hydrological models are used to aid water resource management, yet their treatment of glacier processes is either rudimentary in large applications or linked to fully distributed glacier models that prevent larger model domains. Also, data scarcity in mountainous catchments has hampered the implementation of physically based approaches over entire river catchments. A fully integrated glacier dynamics module was developed for the eco-hydrological model SWIM (SWIM-G) that takes full account of the spatial heterogeneity of mountainous catchments but keeps in line with the semi-distributed disaggregation of the hydrological model. The glacierised part of the catchment is disaggregated into glaciological response units that are based on subbasin, elevation zone and aspect classes. They seamlessly integrate into the hydrological response units of the hydrological model SWIM. Robust and simple approaches to ice flow, avalanching, snow accumulation and metamorphism as well as glacier ablation under consideration of aspect, debris cover and sublimation are implemented in the model, balancing process complexity and data availability. The fully integrated is also capable of simulating a range of other hydrological processes that are common for larger mountainous catchments such as reservoirs, irrigation agriculture and runoff from a diverse soil and vegetation cover. SWIM-G is initialised and calibrated to initial glacier hypsometry, glacier mass balance and river discharge. While the model is intended to be used in medium to large river basins with data-scarce and glacierised headwaters, it is here validated in the data-abundant catchment of the Upper Rhone River, Switzerland and the data-scarce catchment of the Upper Aksu River, Kyrgyzstan/NW China.

1 Introduction

Hydrological modelling and hydrological climate change impact assessments of mountainous and glacierised catchments are plagued with complications and uncertainties (Klemeš, 1990; Schaefli, 2005; Pellicciotti et al., 2012). Strongly heterogeneous processes such as glacier dynamics, orographic precipitation and permafrost are paired with low observation densities, often resulting in severe data scarcity for hydrological modelling. Glaciers have been of particular concern, as their evolution under a changing climate may have significant consequences for downstream water resources (Huss et al., 2008; Immerzeel et al., 2010; Bolch et al., 2012). Representing long-term glacier dynamics in a general-purpose hydrological catchment model has so far been limited (Naz et al., 2014).

Water management of glacierised catchments relies on hydrological models that estimate glacier melt contribution to river discharge of a given glacier cover, often referred to as glacio-hydrological models. Data gaps are overcome by spatial interpolation and integration as well as empirical parametrisations. There is a range of conceptual, semi-distributed models with a long history that incorporate glacier melt successfully and are mainly based on the Degree-Day approach (Quick and Pipes, 1977; Schaefli, 2005; Hagg et al., 2007; Duethmann et al., 2013; Hock, 2005). They perform well over 1–10 year time scales, while being parametrised and calibrated to specific mountainous catchments. There are also some fully distributed and often more physically based models with resolutions of 25–300 m (Finger et al., 2011; Immerzeel et al., 2014; Huss et al., 2010b; Dickerson-Lange and Mitchell, 2014). They are spatially more explicit with more parameter redundancy and higher computational demands. Processes are implemented with more physical meaning, such as the full energy balance at the glacier surface for mass balance accounting. This class of models, however, suffers most from data scarcity, often leading to worse validation results than the former, due to the reliance on driving data (e.g. radiation, albedo etc.) that is not easily interpolated to the model domain.

In addition to glacier mass balance modelling, only a few hydrological models consider ice dynamics, i.e. the lateral redistribution of ice down-slope under the force of gravity. For example, the fully distributed GERM model updates glacier cover annually using an empirical parametrisation of ice thickness changes (Huss et al., 2010b). Some two-dimensional glacier models (without catchment hydrology) have been developed to simulate glacier mass balances and ice dynamics from the glacier to the regional scale (Vieli, 2015; Clarke et al., 2015; Rowan et al., 2015). Fully integrated glacio-hydrological catchment models, however, are rare with the pioneering exception by Naz et al. (2014). They use the shallow ice approximation to evolve glacier surfaces in response to a full energy balance mass balance model and a comprehensive hydrological model at a resolution of 300 m, albeit a catchment of only 422 km^2 in size. Few semi-distributed, conceptual models consider ice dynamics as part of the glacier modelling, but glaciers are only represented as fractional coverage of elevation bands, neglecting the complex terrain in their mass balance and ice flow calculations (e.g. Uhlmann et al., 2013).

Short-comings of current glacio-hydrological models for long-term climate change impact assessments can be loosely divided into problems of a) integration and b) scale:

Integration. Most existing glacio-hydrological models have no or only a simple representation of the remaining catchment hydrology, as it remains a less important factor in small glacierised catchments. However, there is often a considerable distance between the glacierised part of a catchment and the locations where water becomes a socioeconomic and ecological resource. It is in these locations where long-term hydrological observations are recorded that are needed for model calibration. The distance from the glaciers increases the catchment size, increasing the need for more accurate descriptions of the diverse landscape hydrology (e.g. vegetation, groundwater, irrigation agriculture and reservoirs). This is particularly important in long-term studies with drastic glacier changes: Glacier shrinkage exposes more area to solely hydrological processes, while precipitation increase promotes glacier growth but also more runoff in lower-laying areas of the catchment. Similarly, loosely coupled approaches often simulate glacier mass balances and snow cover separately, leading to inconsistencies in the modelling chain.

Scale. Only fully integrated and mostly physically based models have been used to model both glacier evolution and catchment hydrology. Besides their high demand for driving data, they are constrained to relatively small catchments (a few 10s to a few 1000s of square kilometre in size). This is mainly due to their fully distributed nature and the related grid discretisation. In most cases, these models include a computationally intensive, two-dimensional finite-difference approach to ice flow, model runtimes increase drastically with finer resolutions, larger catchments and more sophisticated numerical solutions. The grid resolution is dictated by the complex terrain or the smallest glacier area that is intended to be represented, which puts the maximum grid size to several 100s of meters (Immerzeel et al. (2014) use 500m as the largest found in the literature). While higher resolutions are necessary for the representation of glacier processes, they are unnecessary for hydrological processes in large catchments with sparse observation data.

For long-term assessments of large (partially) glacierised catchments and full mountain ranges, an efficient model is required that integrates a complete description of the catchment hydrology with glacier mass balance and ice dynamics modelling (Naz et al., 2014).

This work's aim is to integrate glacier dynamics and mass balance processes into a general and process-based hydrological model to aid long-term and integrated climate change impact assessments. This will fill the gap between distributed small-scale glacio-hydrological models and large-scale hydrological assessments that ignore or strongly simplify ice dynamics.

In this pursuit, the semi-distributed, eco-hydrological Soil and Water Integrated Model (SWIM Krysanova et al., 1998) was extended by a glacier dynamics module (subsequently called SWIM-G), that includes the important glacier processes. It is tested and validated in the data-scarce Upper Aksu catchment as well as the 'data-abundant' Upper Rhone catchment. While its intended use is primarily for data-scarce catchment, the Upper Rhone catchment serves as a validation case study and to contrast advantages and disadvantages both data conditions offer.

2 Methods

The model integration presented here is based on the idea that proven concepts in hydrological modelling exist (Peel and Blöschl, 2011), while glaciological models are highly specialised and not readily transferable to the catchment scale. Recent advances in glaciological modelling and the emergence of accurate, catchment and region-wide glacier outlines and mass balances (e.g. Fischer et al. (2014, 2015) for Switzerland, Pieczonka and Bolch (2015) for the Central Tien Shan) enable catchment-wide modelling on the glacier scale. In the following, the hydrological model SWIM is briefly outlined followed by more detailed descriptions of the newly implemented glacier processes. The calibration and validation strategy including the two case study catchments are described at the end of this section.

Hydrol. Earth Syst. Sci. Discuss., doi:10.5194/hess-2016-272, 2016
Manuscript under review for journal Hydrol. Earth Syst. Sci.
Published: 16 June 2016

Hydrology and Earth System Sciences
Open Access
Discussions

2.1 The Soil and Water Integrated Model (SWIM)

The Soil and Water Integrated Model (SWIM) is a semi-distributed, process-based, ecohydrological model (Krysanova et al., 1998) with its origins in the semi-distributed model SWAT (Arnold et al., 1993). It was initially developed for long-term climate change impact assessments for medium to large river basins, but has since been developed into a fully integrated ecohydrological model encompassing a number of hydrological and water management processes for both water availability and water quality assessments Hattermann et al. (2011); Huang et al. (2010); Liersch et al. (2012); Koch et al. (2013). Krysanova et al. (2015) provides an overview of the hydrological processes considered and recent advances in its development.

An extended degree-day method is used to simulate snow melt (Huang et al., 2013a, b). It includes a continuous description of ice and water content in the snowpack as well as refreezing and metamorphism according to the approach of Gelfan et al. (2004). As it relies on accurate mean daily temperature, 100 m elevation bands are used to split hydrotopes and to adjust the subbasin mean temperature to the hydrotope elevation by a lapse rate that is catchment specific. The lapse rate varies between -0.3 °C/100m for humid condition and up to -0.9 °C/100m for dry conditions. Precipitation falls as snow if mean temperature falls below a threshold T_s and melts if it exceeds a threshold T_m via the degree-day method (Hock and Holmgren, 2005). Both thresholds are subject to calibration but are generally well-confined to ± 3 °C. The snow module of SWIM provides the main input to the newly developed glacier module, which is described in the following sections.

2.2 Spatial disaggregation of glaciers

SWIM is a semi-distributed, hydrological model with three levels of disaggregation: the basin, subbasins and the hydrotopes. The hydrotopes subdivide the subbasins typically by unique combinations of land cover, soil class and elevation band, but this can be refined by other variables. They provide an adaptive spatial unit depending on the process scale and available data. Taking on this proven hydrological concept, they are here used to represent glaciers. The hydrotopes are used to represent the complex mountainous terrain that determines glacier geometry and distribution by considering slope and aspect classes as well as elevation zones. This type of terrain abstraction is common in geomorphology with established threshold values and classification methods (Bishop et al., 2003; Cronin, 2000; Rasemann et al., 2004), while it is here used with the focus on glacier properties.

In the potential glacier region of the river basin, the hydrotopes are unique combinations of three terrain classifications that are derived from the DEM: *a*) a valley and hillslope class (using a slope threshold), *b*) elevation zones with small intervals in valleys and larger intervals on hillslopes, and *c*) four, regularly spaced aspect classes on hillslopes only. The unique combinations produce a noisy map that needs to be cleaned with a minimum area threshold and successive neighbourhood filling (Figure 1).

Typical elevation zones in hydrological models vary between 20–200 m (Lindström et al., 1997). The variable elevation zone intervals in valleys and hillslopes stems from the desire to have equally sized spatial units. Typical slope values for the two classes should thus govern the choice of intervals. A factor of 10 between valley and hillslope intervals, for example, will lead to equal downslope distances with typical slope angles of 3.9° and 34°. Distinguishing between slope aspect is important to subdivide elevation zones. The aspect classes break these into distinct hillslope units that are more representative of glacial hillslopes than an entire elevation zone and distinguish glaciers with different exposure.

The slope threshold, the elevation intervals, the number of aspect classes and minimum cleaning area are threshold values that can be adapted to the desired level of terrain descretisation and are also dependent on the resolution of the DEM. Here, a slope threshold of $< 15°$, elevation zones of $40\,\mathrm{m}$ in valleys and $400\,\mathrm{m}$ on hillslopes, four aspect classes and a minimum area of $0.5\,\mathrm{km}^2$ is used here. The minimum area threshold limits the model to glaciers larger than this threshold. These representative units resolve the glacial systems of the catchment as well as the hillslopes contributing to glacier accumulation.

Other spatial attributes relevant to the hydrological model are mapped onto the spatial structure of the glacier units, i.e. for each hydrotope the dominant land cover and soil class are used. As soil inventories in mountainous areas mainly apply to valleys (alluvial fans, plateaus) and the hillslopes are mainly composed of bare rock and extremely shallow soils, the soil depth on the hillslope units is reduced to $300\,\mathrm{mm}$ in line with typical soil depths in steep terrain (Dietrich et al., 1995; Heimsath et al., 1999).

2.3 Glacier formation and accumulation

All snow processes are governed by the existing snow module, this includes the description of ice and water content of the snow pack and melt is calculated accordingly. If at the end of the ablation season (defined as the last day of September) snow is left in the hydrotope, it turns into ice if it exceeds the critical height H_c, above which ice flow occurs. H_c is dependent on both slope α and shear stress τ_s, the force the ice needs to overcome to deform under its own weight. Although shear stress varies widely between glaciers and regions, a global average of 10^5 Pa is widely accepted (Cuffey and Paterson, 2010). H_c [m] is determined by the equation:

$$H_c = \frac{\tau_s}{\rho \cdot g \cdot \tan(\alpha)} \tag{1}$$

with glacier ice density ρ ($900\,\mathrm{kg\,m^{-3}}$), gravity g ($9.8066\,\mathrm{m\,s^{-2}}$) and slope angle α [°].

2.4 Ice flow

The routing between the glacier units is calculated similarly to the subbasin routing, i.e. according to the flow direction given in the DEM. Ice flow occurs if the critical height H_c is exceeded; if the thickness decreases below H_c, the ice area of the unit is proportionally decreased to simulate slow terminus recessions. Figure 2 shows the routing between the glacier units in a single subbasin and a valley cross-section of three units. The flow volume Q_i [$\mathrm{m^3}$ w.e. $\mathrm{a^{-1}}$] is based on Glen's Flow Law and the adaptation suggested by Marshall et al. (2011):

$$Q_i = \chi \cdot A_u \cdot H^5 \cdot \tan(\alpha)^3 \tag{2}$$

with area of the glacier unit A_u [$\mathrm{m^2}$], glacier thickness H [m w.e.], slope α [°] and the rheology term χ [$\mathrm{m^{-4}a^{-1}}$] that is subject to calibration. The flux Q_i is routed to the next glacier unit, but is constrained to the volume above the critical height.

Hydrol. Earth Syst. Sci. Discuss., doi:10.5194/hess-2016-272, 2016
Manuscript under review for journal Hydrol. Earth Syst. Sci.
Published: 16 June 2016

Hydrology and Earth System Sciences
Open Access
Discussions

To account for more accurate glacier area changes that in turn have a strong impact on catchment wide glacier melt, the glacier critical height is maintained if melting occurs while the glacier is at this level and instead the fraction of glacier area is reduced, as illustrated in Figure 2b. This simulates the gradual recession of a glacier front up-slope, exposing a decreasing area to melting after the glacier falls below the critical height. The vertical frontal area of the glacier snout needs to be accounted for to avoid the glacier unit to shrink indefinitely without ever disappearing completely. This area is approximated by the glacier height and the squareroot of the unit area. The glacier area of the glacier unit subject to melting A_m [m^2] is given by:

$$A_m = A_u \cdot \frac{H}{H_c} + H_c \cdot \sqrt{A_u} \tag{3}$$

2.5 Avalanching

Avalanching represents a more rapid form of snow and ice redistribution as the majority of the snow or firn column is removed and transported to down-slope. The avalanche-prone areas are identified by a simple slope threshold that is physically based and well constrained to a range of 35–45° (Schweizer et al., 2003) and should be adapted to the observed glacier hypsometry and distribution. If the snow and glacier height exceed the critical height, the snow is accumulated on the remaining fraction of the glacier unit or if the avalanche proportion is greater than 90%, all snow is transported down-slope to the next glacier unit. This upper threshold is needed for numerical stability to avoid large snow masses 'piling up' on small fractions of the glacier unit.

2.6 Glacier melt

The well-tested Degree-Day approach is implemented to simulate glacier melt, as temperature is the least uncertain available climate variable (Hock, 2003). Glacier melt is then collected in a linear reservoir together with liquid precipitation over the glacier, is subject to evaporation and released as glacier discharge Q_g with a delay described by the residence time. This is to simulate the water storage capacity of glaciers and the observed delay of glacier discharge after intensive melting periods (Cuffey and Paterson, 2010). The following equations describe the glacier melt M_g and water outflow Q_w from the linear reservoir V_w:

$$M_g = \begin{cases} \delta_g \cdot T & \text{if } T > 0 \text{ and } H_s = 0 \\ 0 & \text{otherwise} \end{cases} \tag{4}$$

with the Degree-Day factor δ_g [mm °C^{-1} d^{-1}], daily mean temperature T [°C], glacier H_g and snow height H_s.

$$\frac{\delta V_w}{\delta t} = M_g + P_l - E - Q_w \tag{5}$$

$$Q_w = \frac{V_w}{t_r} \tag{6}$$

where evaporation E [mm]; liquid precipitation P_l and residence time t_r [d] ranges between 1–10 days and may be calibrated, for example, using individual melt events without rain. Potential evaporation is calculated by the Priestly-Taylor approach, the standard in SWIM. The glacier water outflow is then subject to the same infiltration and surface runoff processes as liquid precipitation. The valley sediment is described by a highly permeable soil, which saturates quickly resulting in high rates of surface runoff.

Two processes are considered that alter the melt rate over space and time: a) slope aspect and terrain shading (Section 2.8) and b) supraglacial debris cover (Section 2.9). Both processes have been shown to have a significant influence on glacier melt and in turn the spatial distribution of glaciers over longer time periods. Although their governing processes are highly complex, two simple approaches are used to approximate their effect on Degree-Day melting rates, which are spatially distributed.

2.7 Sublimation

In most glacieriesed regions sublimation from the glacier is considered a negligible factor, with rates often far below the error of accumulation rates (Hock and Holmgren, 2005; Gascoin et al., 2011). This is mainly due to the fact that sublimation consumes 8.5 times as much energy (latent heat of sublimation: 2.838×10^6 J kg^{-1} versus latent heat of fusion: 0.334×10^6 J kg^{-1}). In dry and high elevation zones, however, the proportion of energy consumed by sublimation rises to significant levels, suppressing melt rates and meltwater runoff as a result (Zhang et al., 2006; Mölg et al., 2009). High wind speeds and large vapour pressure deficits (or low relative humidity) favour sublimation and are common in high elevations. Modelling day-to-day variations in sublimation rates is only possible with a full energy balance model. However, knowing approximate average ratios of energy used for sublimation, allows the coupling of sublimation with melting. Assuming ablation A is made up of sublimation S and melting M, the energy balance with a sublimation ratio β can be described as follows:

$$M = E \cdot \frac{1-\beta}{L_f} \tag{7}$$

$$S = E \cdot \frac{\beta}{L_s} \tag{8}$$

with the total available energy E [J kg^{-1}] and the latent heat of fusion L_f [J kg^{-1}] and of sublimation L_s [J kg^{-1}]. Using the Degree-Day approach from Equation (4), M can be replaced to solve for E as follows:

$$E = \delta_g \cdot T_+ \cdot \frac{L_f}{1-\beta} \tag{9}$$

Using Equation (8), sublimation can be described by:

$$S = \delta_g \cdot T_+ \cdot \frac{\beta \cdot L_f}{(1-\beta) \cdot L_s} \tag{10}$$

This allows to include sublimation from glaciers using the proven Degree-Day factor approach while only adding a single parameter, that can be estimated from general climatic conditions and sparse energy balance studies. Low observed or calibrated Degree-Day factors are also an indication for high proportions of energy used for sublimation (Zhao et al., 2006; Winkler et al., 2009).

2.8 Slope aspect and terrain shading

Slope aspect and terrain shading reduce the amount of short-wave solar radiation a glacier area receives, which is the predominant driver of glacier melt (Paul, 2010). A first order approximation of this variability is given by the potential sunshine duration per day a slope receives ignoring clouds, a variable readily inferable from a DEM. Although clear-sky solar radiation would provide a more accurate variable (as used in other models, e.g. Huss et al., 2008), it requires additional calibration parameters. Hours of sunlight are computed for both the summer h_s and winter h_w solstice and interpolated for all days in between with a sinus curve (the HBV-ETH model uses a similar sinusoidal differentiation of the Degree-Day factor, but with empirical boundaries, Hock and Holmgren, 2005). The basin-wide Degree-Day factor δ_g is localised by linear scaling as δ_i:

$$h_i = h_w + \frac{h_s - h_w}{2} \cdot \left(1 + \cos\frac{2\pi \cdot i}{365}\right) \tag{11}$$

$$\delta_i = \delta_g \cdot \frac{h_i}{12} \tag{12}$$

where i are the days since the winter solstice, sun hours on day i, on the summer and winter solstice are h_i, h_s, h_w. Although potential sun hours neglect cloud shadowing and the fact that melting is also driven by turbulent heat flux and defuse radiation, it provides an efficient method to vary the melt rate over complex terrain without introducing additional parameters, while the Degree-Day approach allows to calibrate the other melt terms implicitly.

2.9 Debris cover

A supraglacial debris cover has long been shown to first increase glacier ablation up to a thickness of a few centimetres and then significantly decrease ablation (Bozhinskiy et al., 1986; Nicholson and Benn, 2006). The initial increase in melting is caused by the decreased albedo of debris and subsequent thermal conductivity to the glacier ice. This effect, however, is rapidly decreased by the thermal shielding effect of debris layers thicker than a few centimetres. Observing the initial increase has been difficult and including the effect in modelling would require estimating debris thickness with errors smaller then the threshold thickness. Since this is beyond the precision of the model, only the decreasing effect of such a debris layer is considered here.

Several in situ studies have linked debris cover to subdebris ablation rates using a negative exponential relationship (Mattson, 1993; Nicholson and Benn, 2006, e.g. in the Himalaya and several other regions). Considering the measured daily mean temperature, the ablation can be expressed in terms of Degree-Day factors, which vary between region and glacier. One such study has been conducted on the largest glacier of the Tien Shan, the heavily debris-covered South Inylchek glacier, Kyrgyzstan (Hagg et al., 2008). They find the following equation to describe the subdebris melt factor δ_d with increasing debris cover thickness with a correlation of 0.94:

$$\delta_d = \delta_i \cdot e^{-0.0572 \cdot H_d} \tag{13}$$

Hydrology and Earth System Sciences
Open Access
Discussions

with the clean ice melt factor δ_i [mm °C^{-1} d^{-1}], and the debris thickness H_d [cm]. This empirical relationship is employed in the case of the Upper Aksu model, which includes the South Inylchek glacier in its catchment. The clean ice Degree-Day factor is subject to calibration.

As delineating the spatial distribution and estimating the thickness of debris cover over an entire river catchment is near to impossible, let alone knowing its development in the future, a dynamical approximation of the glacier cover was implemented. Supraglacial debris has several origins; deposition of colluvial material, emergence of subglacial moraines and by melt out of englacial debris are the main processes involved (Bolch, 2011). While the first two processes are highly local processes and glacier specific, englacial debris melt out is the only one mainly driven by meteorology and universally applicable to a wider region (with varying intensity between regions). To simulate the evolution of debris produced by this process, an englacial debris concentration approach is implemented (previously proven by Bozhinskiy et al. (1986) in a more complex form). While snow accumulation decreases the concentration, melting increases it and ice flow 'dilutes' the downstream concentration with the one upstream.

An assumed initial debris concentration C_{init} is altered by melting and accumulation in a glacier unit with the specific debris concentration C_g according to the following equation:

$$\frac{\delta C_g}{\delta t} = C_g \cdot (1 + \frac{M_g - H_s}{H_g}) + (C_u - C_g) \cdot \frac{H_q}{H_g}, \quad C_{init} \leq C_g < 1 \tag{14}$$

with glacier thickness H_g, glacier melt M_g, firn accumulation H_s, ice flux height H_q and debris concentration of the upstream unit C_u.

The debris concentration above the initial concentration is assumed to cover the glacier surface. The actual debris height H_d is a fraction of the critical glacier height H_c (see Section 2.3) for simplicity taking account of the slope dependence and the minimum glacier thickness. This is expressed by the following equation:

$$H_d = H_c \cdot (C_g - C_{init}) \tag{15}$$

While this method is a strong approximation of the actual local debris conditions, it reproduces the basin-wide condition of increasing debris cover with increasing melt, typical for low laying glacier snouts. The calibration parameter C_{init} is used to adjust debris thickness to comparable observed values.

2.10 Precipitation correction

Mountainous catchments are highly susceptible to inaccurate precipitation observations due to a) low station density, b) high heterogeneity (i.e. short correlation distances) and orographic precipitation with a measurement bias in valleys. When modelling glacierised catchments, using accurate precipitation (at least on annual basis) is important to achieve realistic glacier mass balances, rather than compensating underestimated precipitation with increased glacier melting. In this regard, glacier models have proven useful tools in finding accurate correction factors and gradients with elevation when a near-glacier equilibrium is assumed or mass balances are known, as was done in Immerzeel et al. (2012) and Immerzeel et al. (2015). Both studies use a simple degree-day glacier melt model to show that measured precipitation underestimates glacier accumulation by factors of 2–10 in multiple glacier catchments of the Indus headwaters.

Where meteorological information has to be extrapolated into great distances both horizontally and/or vertically, a method to correct for orographic precipitation is paramount to the accurate modelling of both the glaciers and the catchment hydrology (Immerzeel et al., 2014; Stisen et al., 2012). Most studies use linear gradients to vary precipitation with elevation over a complex terrain with typical ranges of 0.05–0.5 % m^{-1}. However, representing variance of precipitation as a linear function of elevation is inherently local, highly variable over varying altitude ranges and generally unsuitable for elevations below the reference altitude. For the data-scarce Upper Aksu catchment in this study, precipitation is corrected by a function of altitude taking account of varying gradients and an eventual decrease at very high elevations. The correction factor f_c in Equation (16) remains 1 over lower laying elevations for which observations are available, but increases exponentially up to a maximum gradient a. It then reduces the gradient until a maximum correction c at altitude m is reached and decreases again at higher elevations thereafter.

$$f_c(z) = (c-1) \cdot \exp\left[-\left(\frac{a}{c-1}\right)^2 \cdot (z-m)^2\right] + 1 \tag{16}$$

This is a more dynamic approach than the combination of two linear functions proposed by Immerzeel et al. (2012). c is effectively the greatest correction applied, while the altitude m is the physical limit of the atmosphere to lose more moisture. For the Tien Shan, Aizen et al. (1995) provide approximate values for all three parameters of the correction function.

Since the Upper Rhone catchment has a much higher density of meteorological stations, the above form of altitude-dependent correction was not necessary. Instead, all available precipitation data were interpolated via the Inverse-Distance-Weighting method and corrected by factors published in the Swiss Hydrological Atlas (Sevruk, 1985; Kirchhofer, 2000).

2.11 Glacier initialisation

Glaciers need decades to centuries to reach an equilibrium under a given stable climate. To take account of these long-term dynamics at the start of the modelling period, the ice cover has to be initialised by the model using a representative quasi-stable climate of this length. This ensures consistency between glacier cover and the driving data, as the interpolated climate data is inherently imprecise compared to the observed glacier cover. Also, the model processes and spatial structure are an imperfect representation of actual conditions, so that observed glacier areas and volumes can not be directly used as initial conditions.

For the proposed model, the glacier area and volume are initialised using a climate period in which the glacier mass balance is known to be close to 0, i.e. in a quasi-equilibrium state (Clarke et al., 2015; Marshall et al., 2011). Since this period is in most cases shorter than the time it takes for a glacier to reach an equilibrium, shorter periods are used successively for 200–1000 years. Mass balance records around the world have exhibited balanced or even positive budgets in the 1960's until the mid-1970's (Dyurgerov, 2010; Sorg et al., print October 2012; Dyurgerov and Meier, 1997; WGMS and UNEP, 2008).

This is also true for reference glaciers in and close to the case study catchments of this study: The long-term mass balance records of the Griess glacier in the Rhone catchment show a mean of $-79\,\mathrm{mm\,a^{-1}}$ between 1962–1980. For the Tien Shan, Dyurgerov (2010) puts forward a regional average mass balance that shows an mean balance of $-82\,\mathrm{mm\,a^{-1}}$ between 1960–1975 (also confirmed by Farinotti et al., 2015). These periods were chosen for the initialisation of the glacier cover in the respective catchments.

Hydrol. Earth Syst. Sci. Discuss., doi:10.5194/hess-2016-272, 2016
Manuscript under review for journal Hydrol. Earth Syst. Sci.
Published: 16 June 2016

Hydrology and Earth System Sciences
Open Access
Discussions

Glaciers are never in a perfect equilibrium state, as the two examples above show. But typically, near-stable periods can be identified and the 1960's and 1970's are the latest periods known that also overlap with meteorological observations. Since the model initialisation assumes a perfect equilibrium, the residual mass balance must be represented by a calibration parameter that either adds or subtracts mass from the annual balance during the initialisation period. Clarke et al. (2015) use a similar bias approach in their mass balance model to initialise glaciers of western Canada. The residual mass balance parameter b_r ensures that the equilibrium assumption of the initialisation does not lead to wrong parametrisations of accumulation (precipitation correction) or ablation (glacier melt). The calibration strategy of this and other parameters is discussed in the following section.

2.12 Multi-objective calibration

Constraining the parameters of a glacio-hydrological model is necessarily a multi-objective problem, when both glacier and river discharge observations are available. It is the concurrent simulation of both physical systems that makes it a mutually beneficial exercise at the catchment scale: Accurate glacier behaviour validates the precipitation correction as well as glacier melt for the accurate simulation of discharge and vice versa.

An overview of the parameters (introduced in the previous sections) used for calibration is given in Table 1. The glacier-relevant parameters are mainly calibrated during the glacier initialisation; they are the precipitation correction, the snow and ice melt rates, the ice rheology and the residual mass balance. The most important hydrological parameters are the saturated conductivity correction, evapotranspiration correction and the routing parameters with some less important ones left at typical values. Their ranges are catchment and input data dependent and were tightly constrained by values reported in the literature.

The model is calibrated to daily discharge observations, observed glacier area and catchment-wide, annual mass balances. Four objective functions were chosen to rate the quality of the simulation: The quality of the discharge simulations is given by the commonly used Nash-Satcliff Efficiency (Nash and Sutcliffe, 1970) and the bias in water balance. The model's accuracy in simulating the glacier area is quantified by the Root Mean Square Error (RMSE) between simulated and observed hypsometry. The RMSE is also used to quantify the error in annual, catchment-wide mass balances.

While manually calibrating the model to four objectives is possible, it is a painstaking and time-consuming exercise. After initial manual tests, the widely used automatic calibration algorithm, the Non-dominated Sorting Genetic Algorithm 2 or NSGA-2 (Deb et al., 2002), was chosen to provide multiple parameter sets. NSGA-2 employs evolutionary computation paired with the multi-objective Pareto optimality to rank and select well-performing 'individuals' (i.e. parameter sets). The result is a collection of archived parameter sets that all produce 'good' results by at least objective function. 'Good' here means that no other objective function can be improved without degrading any other objective function, making them all 'Pareto-optimal' (together forming a Pareto front). It is up to the user to choose acceptable trade-offs between them.

A population size of 50 individuals was chosen that are concurrently evaluated over 100 generations, i.e. 5000 evaluations. Considering the 10–13 dimensional parameter space, these do not ensure finding all optimal solutions for the model. However, the method does provide an efficient way to finding some of them within a manageable computing time. The parallel evaluation reduces the calibration time to approximately the number of generations times model runtime, keeping the calibration time to 1–2 days rather than several weeks.

3 Catchments and data

Two catchments similar in size and glacier coverage were chosen to validate the model (Table 2 and Figure 3). The catchment of the Upper Aksu River, Kyrgyzstan/NW China, is a data-scarce catchment typical for mountainous regions in Asia that the model was developed for. A second catchment, that of the Upper Rhone River, Switzerland was chosen to test the model under 'data-abundant' conditions. The data sources used in the model are briefly discussed and listed in Table 3.

3.1 The Upper Tarim basin

The Upper Aksu catchment is located in the Inner Tien Shan mountain range in Central Asia, with the majority of the area in Kyrgyzstan but draining south into the Xinjiang Uighur Autonomous region of NW China. The 12 991 km^2 large catchment has a mean elevation of 3731 m with the highest peak of the Tien Shan, the Jengish Chokuso in Kyrgyz (or Pik Pobedy in Russian or Tömür in Uyghur) at 7439 m. The highest peak is also the source of the largest glacier system of the Tien Shan, the Northern and Southern Inylchek glaciers (Shangguan et al., 2015). The southern branch dams the near-annually outbursting Merzbacher Lake that has been widely discussed in the literature (Ng et al., 2007; Glazirin, 2010; Wortmann et al., 2014). About 45% of the catchment discharge is produced by glacier meltwater (Krysanova et al., 2015) and has been rising over the past 40 years with about 20% found to arise from glacier mass loss since 1975 (Pieczonka and Bolch, 2015).

The catchment's extensive glacier cover with an area of about 2800 km^2 has been shown to recede at a relatively small average rate of about -0.11 ± 0.15 % a^{-1} for the period $\tilde{1}$975 to 2008, while the observed mass balance between 1975 and 2000 was reported to be within the global average at -350 mm w.e. a^{-1}, yet heterogeneously distributed within the basin with only -200 mm w.e. a^{-1} in the high-elevation Inylchek area, but -510 mm w.e. a^{-1} in the northwestern Ak-Shirak range (Pieczonka and Bolch, 2015). A common feature of the large valley glaciers is a thick debris cover as well as terminal ice-cored moraines. The effect on melt rates was researched by Hagg et al. (2008) and is also implemented in the model proposed in this study. The glacier volume and ice thickness distribution was estimated based on the Glabtop2 model introduced by Linsbauer et al. (2012) and modified by Frey et al. (2014) using the filled SRTM DEM and the 1970s glacier inventory as input (cf. Duethmann et al., 2015).

The only long-term, high-altitude meteorological observations are available from a station just west of the catchment (Tien Shan station at 3639 m asl.) with a mean annual precipitation of 320 mm a^{-1} and a mean temperature of -7 °C (Klein Tank et al., 2002) (three precipitation gauge stations were also intermittently active during the 1950's and 1980's). Due to this data scarcity, two available reanalysis datasets were used to drive the model. The WATCH dataset (Weedon et al., 2011) provides a continuous daily timeseries of many climatological variables at a 0.5° spatial resolution. This was complimented with the APHRODITE dataset for it's precipitation station density was shown to be superior to WATCH (Yatagai et al., 2012). The quality and relatively coarse resolution of the climate data make a substantial precipitation correction indispensable, as discussed in Section 2.10.

3.2 The Upper Rhone catchment

The Rhone River originates from the Rhone glacier in southern Switzerland and its catchment has the largest glacier cover in Europe. The focus here is on the Alpine part of the catchment terminating just before Lake Geneva at the gauge station Port du Scex. The catchment incorporates the Alps' largest glacier, Great Aletsch Glacier, in the north-east and many other well studied glaciers in the south. It is dominated by a temperate climate with a strong elevation dependency: While the valley floors receive 500–800 mm a^{-1} of precipitation, elevations above 2000 m receive 2000–3000 mm a^{-1} (Kirchhofer, 2000).

As with the rest of the Alps, the glaciers in the Upper Rhone catchment have seen rapid glacier retreat over the past three decades, but also follow the global trend of near-stable or even advancing conditions in the 1960s and 1970s (Huss et al., 2010a). Since the 1973 until 2010, glacier area has shrunk from 722 km^2 to 569 km^2, a relative change of $-0.57\,\%\,a^{-1}$ (Paul, 2003; Fischer et al., 2014). Mass loss in the Rhone catchment between 1980–2010 was shown to be heterogenous in magnitude ranging from 200–1200 mm w.e. a^{-1} with an average of 590 mm w.e. a^{-1} (Fischer et al., 2015). Griesgletscher, one of two WGMS reference glaciers in the Alps located in the southeast of the catchment (Zemp et al., 2009) has an average mass balance of -1002 mm w.e. a^{-1} over the same period. This long-term mass balance record is scaled by the geodetic catchment-wide mass balance for the calibration of the model.

The Upper Rhone catchment is regulated by 11 high head hydropower dams that were constructed between 1951–1975. A cumulated reservoir capacity of 1186×10^6 m^3 is installed to date up to Lake Geneva (Meile et al., 2010). Although reservoirs are not a focus of this study, it was found essential to represent the largest reservoirs in the model to adequately simulate downstream discharge that is important for the calibration of the glacier model. The four largest dams (Lake Dix, Lake Emosson, Lake Mauvoisin and Lake Moiry; see Figure 3) were implement using SWIM's reservoir model (Koch et al., 2013). In the absence of reservoir discharge data due to the power companies' data restriction, average monthly filling quotas of Switzerland are used that were shown to highly correlate with most of the reservoirs in the catchment (a notable exception is the Lake Dix that has a more complex pumping network) from Schaefli (2005). While monthly average filling quotas do not reproduce the daily variability of the reservoir discharge, it is sufficient to reproduce the storage effect from summer to winter discharge. The effect of Sunday closures of the reservoirs was reduced by excluding them from the observation data. The implementation of the reservoir module also demonstrates the benefits of the glacier assessment within an integrated hydrological model.

The reason for choosing this catchment for the validation of the model is the relative data abundance in comparison to other glacierised catchments: There are eight long-term meteorological stations available with temperature, radiation and humidity observations as well as a further 70 precipitation stations. In addition to that, the region has received extensive research yielding verified results on glaciological development (e.g. Braithwaite and Zhang, 2000; Farinotti et al., 2009; Fischer et al., 2015), climatic variability with elevation (e.g. Sevruk and Mieglitz, 2002; Kirchhofer, 2000) and successful hydrological modelling including glacier melt and large reservoirs (e.g. Rahman et al., 2012; Uhlmann et al., 2013; Fatichi et al., 2015). The research confirms many of the concepts and methods used in the presented model. Rahman et al. (2012) implement the semi-distributed model SWAT to the same model domain. They demonstrate the complexities in modelling this highly glacierised and regulated mountainous catchment focusing on the extensive hydropower network of the Grande Dixence reservoir. Uhlmann et al. (2013)

Hydrol. Earth Syst. Sci. Discuss., doi:10.5194/hess-2016-272, 2016
Manuscript under review for journal Hydrol. Earth Syst. Sci.
Published: 16 June 2016

implement a semi-distributed with conceptual, semi-distributed glacio-hydrological model that has an empirical parameterisation of glacier flow in between elevation zones.

4 Results

From the Pareto-optimal solutions, the 25 best runs were selected. The selection of 'best' results was guided by minimal performance criteria that were then successively increased to yield the best 25. Table 4 provides an overview of the performance for both the hydrological and glaciological objective functions: Median values are given with parameter uncertainty ranges indicated by minimum and maximum values in brackets, i.e. the performance ranges over all 25 runs. The glacier area objective is given in two measures: the sum of absolute errors between the observed and simulated hypsometry and the deviation of in the total area from the observed. Both values are given as fractions of the total observed area for better comparison between the catchments. Simulated mass balances are contrasted by the mass balance given in the respective studies for both regions.

4.1 Hydrological calibration and validation

The daily simulated and observed discharge is shown in Figure 4 (over 3 years for better visibility) together with the day-of-year mean for both the outlet and one interior station. The hydrological model efficiency in the calibration period ranges from 0.60 to 0.90 with a range in bias of the water balance within $\pm 5.3\%$ indicating a good model performance. However, differences in performance reflect the data quality and the impact of water regulation.

In the data-scarce Upper Aksu catchment, the model performance is significantly higher at the outlet station Xiehela with a NSE of 0.81–0.85, while in the much smaller subcatchment Sary-Djaz, it is only 0.60–0.72. This is an indication that poor precipitation data influences the performance stronger the smaller the catchment size. In the data-abundant Rhone catchment, the best performing catchment is that of the smaller Blatten station with 0.85–0.90 in NSE. The outlet station Port du Scex, however, shows a significant decline in performance with 0.60–0.68. This is most probably due to the many reservoirs that were only implemented on an average monthly basis, although day-to-day fluctuations (e.g. reduced flows on Sundays) are clearly visible (Figure 4). This performance pattern is repeated in the divergence from calibration to validation period; the performance of the Sary-Djaz catchment and the Port du Scex catchment is degrading more than at the other stations, but remains within acceptable limits (NSE 0.58–0.72, bias -11–+5%).

4.2 Glacier initialisation

The objective of the initialisation was to optimise the catchment parameters (mainly, the precipitation correction, ice rheology and the residual mass balance) to match the total catchment glacier area and volume as well as the elevation distribution (hypsometry) of glaciers in the individual subcatchments. An initialisation period of 300 years seemed to be sufficient to reach stability and is within the range of time length used in previous studies (Marshall et al., 2011; Naz et al., 2014).

The catchment-wide observed areas and estimated volumes are matched well by the modelled development of both area and volume over the initialisation period (Figure 5) and helped to rigorously correct the precipitation in conjunction with the observed and simulated catchment discharge (discussed above). While uncertainties in the estimated 'observed' volumes (modelled by Duethmann et al. (2015) for the Upper Aksu catchment and Linsbauer et al. (2012) for the Rhone catchment) undoubtedly exist, the initialised volume is mainly controlled by the rheology parameter of the ice flow equation and the assumed shear stress of 10^5Pa.

The area hypsometry is reproduced well by the model in both catchments (Figure 6). The sum of absolute residuals ranges from 7.2 to 31.2% of the total glacier area, while total area error is within -13.8–18.5 %. The largest mismatches exist in the data-scarce Sary-Djaz catchment, where insufficient driving data is likely affecting the accurate simulation of glacier area distributions. Discrepancies also exist in the elevation range with the largest glacier cover where the model overestimates cover in individual elevation zones by up to 25 % in the Upper Aksu catchment and by up to 18 % in the Rhone catchment.

4.3 Mass balances and area changes

The simulated mass balance was calibrated against reference glacier mass balance records, that were scaled by the catchment-wide geodetic mass balances provided by Pieczonka and Bolch (2015) for the Upper Aksu and by Fischer et al. (2015) for the Upper Rhone catchment. The comparison of both simulated and 'observed' mass balances are shown in Figure 8 including the parameter uncertainty range. Simulated and observed annual mass balances are generally in good agreement (Table 4). The parameter uncertainty ranges in the Upper Aksu catchment are at 0.03–0.04 m w.e. a^{-1} significantly smaller than the error of observations. This is not the case in the Upper Rhone catchment, where the parameter uncertainty range is 0.14–0.16 m w.e. a^{-1} and comparable to the uncertainties of observations. This is due to the fact that Fischer et al. (2015) used higher resolution elevation data (25m, DHM25 and SwissAlti3d), while Pieczonka and Bolch (2015) relied on the SRTM3 DEM (90m resolution) and Hexagon KH-9 stereo data.

Glacier area changes are over the simulation period 1970–2000 in the Upper Aksu and 1980–2010 in the Upper Rhone catchment are shown in Figure 7. They are not part of the calibration, but are compared to geodetic area change values from the literature. There is a good agreement in the Upper Aksu catchment where the parameter uncertainty range fully overlaps the error range of the observations. In the Upper Rhone, the observed shrinkage is slightly higher, but the uncertainty ranges still overlap. The area changes in the much smaller Blatter catchment (Great Aletsch glacier), are significantly smaller than the catchment-wide values. This is in line with the catchment's mean ice thickness of 115 m Linsbauer et al. (2012) and large glacier tongue that make it less sensitive to area changes despite strong mass losses.

4.4 Annual discharge

The hydrological effects of glacier changes are most evident in long-term river discharge. Trends in annual discharge may reflect changes in the glaciers' mass balance but also reflect changes in precipitation. For example, Pieczonka and Bolch (2015) estimate that 20% of discharge increases in the Upper Aksu catchment are due to the glacier imbalance. Glacio-hydrological models are able to decompose those trends to understand changes in river discharge and project possible 'peak discharge' due to glacier decline.

Figure 9 shows annual runoff (annual discharge divided by catchment area) together with precipitation and glacier melt over the 30-year simulation period of the most glacierised catchments of both rivers terminated by Xiehela and Blatten station. Both show a good modelling fit including reproduced trends. However, comparing both catchments also exposes the data quality; the inter-annual variations are reproduced much better in the Upper Rhone and show some larger deviations in the 1990's in the Upper Aksu. This coincides with the decline in precipitation observations that contributed to the APHRODITE reanalysis set with the collapse of the Soviet Union.

Figure 9 also shows annual precipitation and glacier melt distributed over the catchment area (not to be confused with mass balance, i.e. accumulation-melt over the glacier area). Both variables are the principle drivers of inter-annual variability of discharge, as their magnitudes are indicative of the year's climate. The increasing discharge in the Upper Aksu in the last 4 years is caused by both increasing glacier melt and precipitation, for example. Similarly, the increasing trend in discharge at the Blatten (Upper Rhone) station is driven by increasing glacier melt in the 2000s, while precipitation is generally lower than in the previous two decades (hence the strongly negative mass balances). Comparing glacier melt to discharge also highlights the importance of the glaciers in the catchment: The mean glacier melt to discharge ratio is 44% and 43% in the Xiehela and Blatten catchment respectively, although their glacierisation vary significantly with 22% and 57%, respectively.

5 Discussion

SWIM-G, the model presented here bridges the gap between semi-distributed, empirical glacio-hydrological catchment models and fully distributed and more physically based models for small scales. It includes a representation of individual glaciers on the catchment scale without being computationally too demanding and excessively precise. The model integrates ice flow over the spatially adaptive glaciological response units, avoiding computationally expensive finite difference schemes such as Clarke et al. (2015) is using. It represents glacier dynamics of individual glaciers as distributed glacio-hydrological models have done, such as Naz et al. (2014) and Immerzeel et al. (2011), but can do so for much larger catchments at an intermediate resolution appropriate for the catchment hydrology. Previous semi-distributed or empirical approaches to bridge this scale gap such as Uhlmann et al. (2013) and Huss et al. (2010a) have made important advances in this regard, yet do not include a process-based description of glacier dynamics on an individual glacier basis. Some other important glaciological or hydrological processes (e.g. debris cover, sublimation, reservoirs) are so far also missing in these or similar models.

Hydrological modelling of larger glacierised catchments is plagued with data scarcity, often yielding results with high uncertainty. However, recent advances in glaciological remote sensing (Gardelle et al., 2012; Fischer et al., 2015; Pieczonka and Bolch, 2015), in the modelling of climatic parameters (e.g. Maussion et al., 2013; Immerzeel et al., 2015) and the increasing availability of glaciological baseline data have helped to overcome the data gaps. More glacier outlines, mass balance and glacier thickness data from the global terrestrial network for glaciers (www.gtn-g.org) and other databases have become available to modellers. The model presented here attempts to incorporate these advances. It is calibrated not only to measured discharge, but also to glacier distribution and observed mass balance. A larger number and more diverse observations constrain the parameter ranges greatly, which is especially important for those parameters with the largest effects on discharge, i.e.

precipitation correction and glacier melt. Our multi-objective calibration scheme reduces the overall uncertainty of discharge simulations in mountainous catchments with insufficient observations and has been achieved before with similar approaches, such as using remotely sensed snow cover data in conjunction with discharge (Duethmann et al., 2014), the output of regional climate models as weights for a discharge-based precipitation correction (Duethmann et al., 2014) or a precipitation correction solely based on a glacier equilibrium assumption (Immerzeel et al., 2012). Thus, the glacier dynamics module integrated into the hydrological model SWIM and the multi-objective calibration procedure are specifically adapted to such data-scarce catchments.

Another approach to overcome the data scarcity and to also formulate a comprehensive representation of glacier processes is the use of expert parameters, i.e. parameters that are only constrained by expert knowledge, empirical values or point-based measurements (also known as soft information) (Winsemius et al., 2009). For example, the ratio of energy consumed by sublimation or the debris concentration in glaciers are constrained by values reported in the literature that are transferred to the catchments' climates. Similarly, the thresholds used for the spatial disaggregation (elevation zone interval, hillslope threshold, cleaning threshold) are empirical values and depend on the desired level of detail. These parameters are difficult to calibrate because they have little or indirect influences on the calibration objectives and may be easily compensated for by other more dominant parameters (Refsgaard, 1997). They are mostly unique to a particular catchment but constrained by ranges reported in the literature or by model results that are not part of the calibration. While using these parameters leads to a high risk of parameter equifinality and may seem like excessive complexity with high uncertainty (Beven, 2006), they are intended to make the model more robust on longer time scales (i.e. 30 to 100 years) and physically more complete than other empirical and conceptual models of mountain hydrology (Merz et al., 2011). The use of expert parameters allows the scarce information about not systematically observed processes to be included in the modelling, a type of parameter upscaling (Blöschl and Sivapalan, 1995) that is warranted where little to no data exists (Dornes et al., 2008; Krogh et al., 2014). In case more observations of driving variables exist, the model can be extended to more physically based approaches of glacier processes, such as calculating the full energy balance for ablation or the inclusion of an explicit glacier sliding term (e.g. Wertman's sliding law in Immerzeel et al., 2011). However, this would only yield better results if reliable driving data for these approaches (radiation, humidity etc.) are available and can be spatially distributed over the entire catchment.

An important process considered in our model is the evolution of debris cover in response to glacier mass changes. This introduces a much discussed negative feedback into modelling of glaciers under climate change, i.e. the increased shielding of ice as glaciers retreat (Scherler et al., 2011; Kirkbride and Deline, 2013). The implementation here is a starting point for a more general treatment of debris on glaciers because so far the model only considers the relative effect of a negative mass balance on melt rates while absolute debris thickness is unknown on the catchment scale. The approach could be further developed by initialising debris cover along with the ice cover, effectively modelling debris thickness that could be verified against point observations. However, this would require finding a debris equilibrium between debris production and fallout rates. Although several processes governing debris production and deposition are understood (e.g. Hambrey et al., 2008), they have not been systematically described and the implementation has just started (e.g. Rowan et al., 2015) and requires further research. We also did not consider the influence of ice cliffs or supraglacial lakes on glacier melt although they occur frequently on debris-covered glaciers. These hot spots of glacier melt may be significant on some glaciers but are of much less importance than the shielding effect of debris cover (Sakai et al., 1998, 2000; Juen et al., 2014). It is nearly impossible to predict their occurrence, persistence and size at a catchment level as they are mostly erratic features. Similarly erratic processes also unconsidered are wind drifted snow and glacier surges. The limited influence on the catchment hydrology and glacier evolution clearly does not justify the difficulties of implementation and the added uncertainties. However, testing and including more debris processes may be part of future additions to the model.

The successful validation in the two case study catchments has shown that our model is transferable to a range of glacierised catchments. This is especially due to the following four aspects: a) the adaptive and cross-scale spatial disaggregation, b) the process-based and comprehensive process implementation, c) the flexibility in required driving data with emphasis on data scarcity as well as d) the wide applicability of the hydrological model SWIM. Its primary purpose will be to serve as a tool for integrated climate change impact assessments of glaciological and hydrological changes, making use of the climate change scenarios, such as the scenario ensembles of CMIP5 (Taylor et al., 2011) of global climate models or regional scenarios from the CORDEX initiative (Giorgi and Gutowski, 2015).

6 Conclusions

A new catchment-wide glacier model was developed and integrated into the hydrological model SWIM (SWIM-G). It covers all major glacier processes including glacier dynamics, debris melt-out and sublimation. This ensures robustness over long timescales and a range of climatic and glaciological settings, although it was primarily developed for data-scarce catchments of High Asia. The new approach to representing individual glaciers and their ice dynamics in a hydrological model bridges the gap between distributed, physically based glacier dynamics models – that are typically only applicable to single glaciers or small glacier groups – and large-scale empirical glacio-hydrological models. This allows for accurate and integrated glaciological and hydrological assessments of entire, highly glacierised catchments. The intermediate complexity enables ensemble modelling approaches for calibration and scenario analysis by radically reducing computing time compared to fully distributed glacier models.

SWIM-G was implemented and validated in a data-scarce catchment in Kyrgyzstan/NW China and a data-abundant catchment and Switzerland. The calibration yielded good results compared to both discharge and glaciological observations, but performance depends on data quality; precipitation observations in particular. The model was automatically calibrated using a multi-objective evolutionary optimisation that is widely used in hydrological modelling. The parameter uncertainty is comparable to uncertainties of glaciological observations (e.g. glaciological or geodetic area and mass balance observations) but may become large over longer simulation periods due to the variable initialisations. In data-scarce catchments, the model highlights the need for precipitation correction and is able to inform the method of correction by initialising ice cover and calibrating the model using discharge, glacier distribution and glacier mass balance in the multi-objective calibration procedure. The model helps to prevent overestimations of glacier melt in-lieu for negative biases in precipitation observations that are ubiquitous in mountainous catchments. The application to the arid Upper Aksu catchment shows that adequately simulating glacier dynamics (including accurate rates of accumulation and ablation) is vital to properly model this and similar river basins due to their high contribution of glacier melt to discharge. The medium complexity of the developed glacio-hydrological model means that the model is well adapted to large, partially glacierised and data-scarce catchments, as they are often found in High Asia and other mountain ranges of the world. Its main purpose is to serve as a model for long-term glacio-hydrological climate change impact assessments of IPCC scenarios for the 21st century.

Acknowledgements. This study was conducted within the project SuMaRiO (Sustainable Management of River Oases along the Tarim River; http://www.sumario.de/), funded by the German Federal Ministry of Education and Research (BMBF grants 01LL0918J and 01LL0918B). T. Bolch acknowledges funding by Deutsche Forschungsgemeinschaft (DFG, Code BO3199/2-1).

References

Aizen, V., Aizen, E., and Melack, J.: Climate, snow cover, glaciers, and runoff in the Tien Shan, Central Asia, JAWRA Journal of the American Water Resources Association, 31, 1113–1129, doi:10.1111/j.1752-1688.1995.tb03426.x, 1995.

Arnold, J. G., Allen, P. M., and Bernhardt, G.: A comprehensive surface-groundwater flow model, Journal of Hydrology, 142, 47–69, doi:10.1016/0022-1694(93)90004-S, 1993.

Beven, K.: A manifesto for the equifinality thesis, Journal of Hydrology, 320, 18–36, doi:10.1016/j.jhydrol.2005.07.007, 2006.

Bishop, M. P., Shroder Jr., J. F., and Colby, J. D.: Remote sensing and geomorphometry for studying relief production in high mountains, Geomorphology, 55, 345–361, doi:10.1016/S0169-555X(03)00149-1, 2003.

Blöschl, G. and Sivapalan, M.: Scale issues in hydrological modelling: A review, Hydrological Processes, 9, 251–290, doi:10.1002/hyp.3360090305, 1995.

Bolch, T.: Debris, in: Encyclopedia of Snow, Ice and Glaciers, edited by Singh, V. P., Singh, P., and Haritashya, U. K., Encyclopedia of Earth Sciences Series, pp. 176–178, Springer Netherlands, 2011.

Bolch, T., Kulkarni, A., Kääb, A., Huggel, C., Paul, F., Cogley, J. G., Frey, H., Kargel, J. S., Fujita, K., Scheel, M., Bajracharya, S., and Stoffel, M.: The State and Fate of Himalayan Glaciers, Science, 336, 310–314, doi:10.1126/science.1215828, 2012.

Bozhinskiy, A., Krass, M., and Popovnin, V.: Role of debris cover in the thermal physics of glaciers, Journal of Glaciology, 32, 255–266, 1986.

Braithwaite, R. J. and Zhang, Y.: Sensitivity of mass balance of five Swiss glaciers to temperature changes assessed by tuning a degree-day model, Journal of Glaciology, 46, 7–14, doi:10.3189/172756500781833511, 2000.

Clarke, G. K. C., Jarosch, A. H., Anslow, F. S., Radić, V., and Menounos, B.: Projected deglaciation of western Canada in the twenty-first century, Nature Geoscience, advance online publication, doi:10.1038/ngeo2407, 2015.

Cronin, T.: Classifying hills and valleys in digitized terrain, Photogrammetric engineering and remote sensing, 66, 1129–1137, 2000.

Cuffey, K. M. and Paterson, W. S. B.: The physics of glaciers, Elsevier, Amsterdam, 00292, 2010.

Deb, K., Pratap, A., Agarwal, S., and Meyarivan, T.: A fast and elitist multiobjective genetic algorithm: NSGA-II, IEEE Transactions on Evolutionary Computation, 6, 182–197, doi:10.1109/4235.996017, 2002.

Dickerson-Lange, S. E. and Mitchell, R.: Modeling the effects of climate change projections on streamflow in the Nooksack River basin, Northwest Washington, Hydrological Processes, 28, 5236–5250, doi:10.1002/hyp.10012, 2014.

Dietrich, W. E., Reiss, R., Hsu, M.-L., and Montgomery, D. R.: A process-based model for colluvial soil depth and shallow landsliding using digital elevation data, Hydrological Processes, 9, 383–400, doi:10.1002/hyp.3360090311, 1995.

Dornes, P. F., Pomeroy, J. W., Pietroniro, A., Carey, S. K., and Quinton, W. L.: Influence of landscape aggregation in modelling snow-cover ablation and snowmelt runoff in a sub-arctic mountainous environment, Hydrological Sciences Journal, 53, 725–740, doi:10.1623/hysj.53.4.725, 2008.

Duethmann, D., Zimmer, J., Gafurov, A., Güntner, A., Kriegel, D., Merz, B., and Vorogushyn, S.: Evaluation of areal precipitation estimates based on downscaled reanalysis and station data by hydrological modelling, Hydrol. Earth Syst. Sci., 17, 2415–2434, doi:10.5194/hess-17-2415-2013, 2013.

Duethmann, D., Peters, J., Blume, T., Vorogushyn, S., and Güntner, A.: The value of satellite-derived snow cover images for calibrating a hydrological model in snow-dominated catchments in Central Asia, Water Resources Research, 50, 2002–2021, doi:10.1002/2013WR014382, 2014.

Hydrol. Earth Syst. Sci. Discuss., doi:10.5194/hess-2016-272, 2016
Manuscript under review for journal Hydrol. Earth Syst. Sci.
Published: 16 June 2016

Duethmann, D., Bolch, T., Farinotti, D., Kriegel, D., Vorogushyn, S., Merz, B., Pieczonka, T., Jiang, T., Su, B., and Güntner, A.: Attribution of streamflow trends in snow- and glacier melt dominated catchments of the Tarim River, Central Asia, Water Resources Research, pp. 4727–4750, doi:10.1002/2014WR016716, 2015.

Dyurgerov, M. B.: Reanalysis of glacier changes: from the IGY to the IPY, 1960-2008, no. 108 in Data of Glaciological Studies, Glaciological Association, Geographical Institute of the Russian Academy of Sciences, Moscow, 2010.

Dyurgerov, M. B. and Meier, M. F.: Mass Balance of Mountain and Subpolar Glaciers: A New Global Assessment for 1961-1990, Arctic and Alpine Research, 29, 379–391, doi:10.2307/1551986, 1997.

FAO: Crop calendar, http://www.fao.org/agriculture/seed/cropcalendar/, 2011.

Farinotti, D., Huss, M., Bauder, A., and Funk, M.: An estimate of the glacier ice volume in the Swiss Alps, Global and Planetary Change, 68, 225–231, doi:10.1016/j.gloplacha.2009.05.004, 2009.

Farinotti, D., Longuevergne, L., Moholdt, G., Duethmann, D., Mölg, T., Bolch, T., Vorogushyn, S., and Güntner, A.: Substantial glacier mass loss in the Tien Shan over the past 50 years, Nature Geoscience, 8, 716–722, doi:10.1038/ngeo2513, 2015.

Fatichi, S., Rimkus, S., Burlando, P., Bordoy, R., and Molnar, P.: High-resolution distributed analysis of climate and anthropogenic changes on the hydrology of an Alpine catchment, Journal of Hydrology, 525, 362–382, doi:10.1016/j.jhydrol.2015.03.036, 2015.

Finger, D., Pellicciotti, F., Konz, M., Rimkus, S., and Burlando, P.: The value of glacier mass balance, satellite snow cover images, and hourly discharge for improving the performance of a physically based distributed hydrological model, Water Resources Research, 47, W07 519, doi:10.1029/2010WR009824, 2011.

Fischer, M., Huss, M., Barboux, C., and Hoelzle, M.: The New Swiss Glacier Inventory SGI2010: Relevance of Using High-Resolution Source Data in Areas Dominated by Very Small Glaciers, Arctic, Antarctic, and Alpine Research, 46, 933–945, doi:10.1657/1938-4246-46.4.933, 2014.

Fischer, M., Huss, M., and Hoelzle, M.: Surface elevation and mass changes of all Swiss glaciers 1980–2010, The Cryosphere, 9, 525–540, doi:10.5194/tc-9-525-2015, 2015.

Frey, H., Machguth, H., Huss, M., Huggel, C., Bajracharya, S., Bolch, T., Kulkarni, A., Linsbauer, A., Salzmann, N., and Stoffel, M.: Estimating the volume of glaciers in the Himalayan–Karakoram region using different methods, The Cryosphere, 8, 2313–2333, doi:10.5194/tc-8-2313-2014, 2014.

Friedl, M. A., McIver, D. K., Hodges, J. C. F., Zhang, X. Y., Muchoney, D., Strahler, A. H., Woodcock, C. E., Gopal, S., Schneider, A., Cooper, A., Baccini, A., Gao, F., and Schaaf, C.: Global land cover mapping from MODIS: algorithms and early results, Remote Sensing of Environment, 83, 287–302, doi:10.1016/S0034-4257(02)00078-0, 2002.

Gardelle, J., Berthier, E., and Arnaud, Y.: Slight mass gain of Karakoram glaciers in the early twenty-first century, Nature Geoscience, 5, 322–325, doi:10.1038/ngeo1450, 2012.

Gascoin, S., Kinnard, C., Ponce, R., Lhermitte, S., MacDonell, S., and Rabatel, A.: Glacier contribution to streamflow in two headwaters of the Huasco River, Dry Andes of Chile, The Cryosphere, 5, 1099–1113, doi:10.5194/tc-5-1099-2011, 2011.

Gelfan, A., Pomeroy, J., and Kuchment, L.: Modeling forest cover influences on snow accumulation, sublimation, and melt, Journal of Hydrometeorology, 5, 785–803, 2004.

Giorgi, F. and Gutowski, W. J.: Regional Dynamical Downscaling and the CORDEX Initiative, Annual Review of Environment and Resources, 40, 467–490, doi:10.1146/annurev-environ-102014-021217, 2015.

Glazirin, G.: A century of investigations on outbursts of the ice-dammed Lake Merzbacher (Central Tien Shan), Austrian Journal of Earth Sciences, 103, 171–179, 2010.

Hydrol. Earth Syst. Sci. Discuss., doi:10.5194/hess-2016-272, 2016
Manuscript under review for journal Hydrol. Earth Syst. Sci.
Published: 16 June 2016

GRDC: The Global Runoff Data Centre, Tech. rep., Bundesanstalt für Gewässerkunde, 56068 Koblenz, Germany, 2016.

Hagg, W., Braun, L. N., Kuhn, M., and Nesgaard, T. I.: Modelling of hydrological response to climate change in glacierized Central Asian catchments, Journal of Hydrology, 332, 40–53, doi:10.1016/j.jhydrol.2006.06.021, 2007.

Hagg, W., Mayer, C., Lambrecht, A., and Helm, A.: Sub-Debris Melt Rates on Southern Inylchek Glacier, Central Tian Shan, Geografiska Annaler: Series A, Physical Geography, 90, 55–63, doi:10.1111/j.1468-0459.2008.00333.x, 2008.

Hambrey, M. J., Quincey, D. J., Glasser, N. F., Reynolds, J. M., Richardson, S. J., and Clemmens, S.: Sedimentological, geomorphological and dynamic context of debris-mantled glaciers, Mount Everest (Sagarmatha) region, Nepal, Quaternary Science Reviews, 27, 2361–2389, doi:10.1016/j.quascirev.2008.08.010, 2008.

Hattermann, F., Weiland, M., Huang, S., Krysanova, V., and Kundzewicz, Z.: Model-Supported Impact Assessment for the Water Sector in Central Germany Under Climate Change—A Case Study, Water Resources Management, 25, 3113–3134, doi:10.1007/s11269-011-9848-4, 2011.

Heimsath, A. M., E. Dietrich, W., Nishiizumi, K., and Finkel, R. C.: Cosmogenic nuclides, topography, and the spatial variation of soil depth, Geomorphology, 27, 151–172, doi:10.1016/S0169-555X(98)00095-6, 1999.

Hock, R.: Temperature index melt modelling in mountain areas, Journal of Hydrology, 282, 104–115, doi:10.1016/S0022-1694(03)00257-9, 00406, 2003.

Hock, R.: Glacier melt: a review of processes and their modelling, Progress in Physical Geography, 29, 362 –391, doi:10.1191/0309133305pp453ra, 2005.

Hock, R. and Holmgren, B.: A distributed surface energy-balance model for complex topography and its application to Storglaciären, Sweden, Journal of Glaciology, 51, 25–36, doi:10.3189/172756505781829566, 2005.

Huang, S., Krysanova, V., Österle, H., and Hattermann, F. F.: Simulation of spatiotemporal dynamics of water fluxes in Germany under climate change, Hydrological Processes, 24, 3289–3306, doi:10.1002/hyp.7753, 2010.

Huang, S., Hattermann, F. F., Krysanova, V., and Bronstert, A.: Projections of climate change impacts on river flood conditions in Germany by combining three different RCMs with a regional eco-hydrological model, Climatic Change, 116, 631–663, doi:10.1007/s10584-012-0586-2, 2013a.

Huang, S., Krysanova, V., and Hattermann, F. F.: Projection of low flow conditions in Germany under climate change by combining three RCMs and a regional hydrological model, Acta Geophysica, 61, 151–193, doi:10.2478/s11600-012-0065-1, 2013b.

Huss, M., Farinotti, D., Bauder, A., and Funk, M.: Modelling runoff from highly glacierized alpine drainage basins in a changing climate, Hydrological Processes, 22, 3888–3902, doi:10.1002/hyp.7055, 2008.

Huss, M., Hock, R., Bauder, A., and Funk, M.: 100-year mass changes in the Swiss Alps linked to the Atlantic Multidecadal Oscillation, Geophysical Research Letters, 37, L10 501, doi:10.1029/2010GL042616, 00077, 2010a.

Huss, M., Usselmann, S., Farinotti, D., and Bauder, A.: Glacier mass balance in the south-eastern Swiss Alps since 1900 and perspectives for the future, Erdkunde, 64, 119–140, 00025, 2010b.

Immerzeel, W. W., van Beek, L. P. H., and Bierkens, M. F. P.: Climate Change Will Affect the Asian Water Towers, Science, 328, 1382–1385, doi:10.1126/science.1183188, 2010.

Immerzeel, W. W., van Beek, L. P. H., Konz, M., Shrestha, A. B., and Bierkens, M. F. P.: Hydrological response to climate change in a glacierized catchment in the Himalayas, Climatic Change, 110, 721–736, doi:10.1007/s10584-011-0143-4, 2011.

Immerzeel, W. W., Pellicciotti, F., and Shrestha, A. B.: Glaciers as a Proxy to Quantify the Spatial Distribution of Precipitation in the Hunza Basin, Mountain Research and Development, 32, 30–38, doi:10.1659/MRD-JOURNAL-D-11-00097.1, 00023, 2012.

Immerzeel, W. W., Petersen, L., Ragettli, S., and Pellicciotti, F.: The importance of observed gradients of air temperature and precipitation for modeling runoff from a glacierized watershed in the Nepalese Himalayas, Water Resources Research, 50, 2212–2226, doi:10.1002/2013WR014506, 00005, 2014.

Immerzeel, W. W., Wanders, N., Lutz, A. F., Shea, J. M., and Bierkens, M. F. P.: Reconciling high-altitude precipitation in the upper Indus basin with glacier mass balances and runoff, Hydrol. Earth Syst. Sci., 19, 4673–4687, doi:10.5194/hess-19-4673-2015, 2015.

Jarvis, A., Reuter, H., Nelson, A., and Guevara, E.: Hole-filled seamless SRTM data, 2007.

Juen, M., Mayer, C., Lambrecht, A., Han, H., and Liu, S.: Impact of varying debris cover thickness on ablation: a case study for Koxkar Glacier in the Tien Shan, The Cryosphere, 8, 377–386, doi:10.5194/tc-8-377-2014, 2014.

Kirchhofer, W., ed.: Klimaatlas der Schweiz, Schweizerische Meteorologische Anstalt, Wabern, 2000.

Kirkbride, M. P. and Deline, P.: The formation of supraglacial debris covers by primary dispersal from transverse englacial debris bands, Earth Surface Processes and Landforms, 38, 1779–1792, doi:10.1002/esp.3416, 2013.

Klein Tank, A. M. G., Wijngaard, J. B., Können, G. P., Böhm, R., Demarée, G., Gocheva, A., Mileta, M., Pashiardis, S., Hejkrlik, L., Kern-Hansen, C., Heino, R., Bessemoulin, P., Müller-Westermeier, G., Tzanakou, M., Szalai, S., Pálsdóttir, T., Fitzgerald, D., Rubin, S., Capaldo, M., Maugeri, M., Leitass, A., Bukantis, A., Aberfeld, R., van Engelen, A. F. V., Forland, E., Mietus, M., Coelho, F., Mares, C., Razuvaev, V., Nieplova, E., Cegnar, T., Antonio López, J., Dahlström, B., Moberg, A., Kirchhofer, W., Ceylan, A., Pachaliuk, O., Alexander, L. V., and Petrovic, P.: Daily dataset of 20th-century surface air temperature and precipitation series for the European Climate Assessment, International Journal of Climatology, 22, 1441–1453, doi:10.1002/joc.773, 2002.

Klemeš, V.: The modelling of mountain hydrology: the ultimate challenge, in: Hydrology of mountainous areas, vol. 190, pp. 29–43, IAHS, 1990.

Koch, H., Liersch, S., and Hattermann, F. F.: Integrating water resources management in eco-hydrological modelling, Water Science & Technology, 67, doi:10.2166/wst.2013.022, 2013.

Krogh, S. A., Pomeroy, J. W., and McPhee, J.: Physically Based Mountain Hydrological Modeling Using Reanalysis Data in Patagonia, Journal of Hydrometeorology, 16, 172–193, doi:10.1175/JHM-D-13-0178.1, 2014.

Krysanova, V., Müller-Wohlfeil, D., and Becker, A.: Development and test of a spatially distributed hydrological/water quality model for mesoscale watersheds, Ecological Modelling, 106, 261–289, doi:10.1016/S0304-3800(97)00204-4, 00306, 1998.

Krysanova, V., Wortmann, M., Bolch, T., Merz, B., Duethmann, D., Walter, J., Huang, S., Tong, J., Buda, S., and Kundzewicz, Z. W.: Analysis of current trends in climate parameters, river discharge and glaciers in the Aksu River basin (Central Asia), Hydrological Sciences Journal, 60, 566–590, doi:10.1080/02626667.2014.925559, 2015.

Liersch, S., Cools, J., Kone, B., Koch, H., Diallo, M., Reinhardt, J., Fournet, S., Aich, V., and Hattermann, F.: Vulnerability of rice production in the Inner Niger Delta to water resources management under climate variability and change, Environmental Science & Policy, doi:10.1016/j.envsci.2012.10.014, 00003, 2012.

Lindström, G., Johansson, B., Persson, M., Gardelin, M., and Bergström, S.: Development and test of the distributed HBV-96 hydrological model, Journal of Hydrology, 201, 272–288, doi:10.1016/S0022-1694(97)00041-3, 1997.

Linsbauer, A., Paul, F., and Haeberli, W.: Modeling glacier thickness distribution and bed topography over entire mountain ranges with GlabTop: Application of a fast and robust approach, Journal of Geophysical Research: Earth Surface, 117, F03 007, doi:10.1029/2011JF002313, 2012.

Marshall, S. J., White, E. C., Demuth, M. N., Bolch, T., Wheate, R., Menounos, B., Beedle, M. J., and Shea, J. M.: Glacier Water Resources on the Eastern Slopes of the Canadian Rocky Mountains, Canadian Water Resources Journal / Revue canadienne des ressources hydriques, 36, 109–134, doi:10.4296/cwrj3602823, 00027, 2011.

Mattson, L.: Ablation on debris covered glaciers: an example from the Rakhiot Glacier, Panjab, Himalaya, IAHS publication, 218, 289–296, 00125, 1993.

Maussion, F., Scherer, D., Mölg, T., Collier, E., Curio, J., and Finkelnburg, R.: Precipitation Seasonality and Variability over the Tibetan Plateau as Resolved by the High Asia Reanalysis, Journal of Climate, 27, 1910–1927, doi:10.1175/JCLI-D-13-00282.1, 2013.

Meile, T., Boillat, J.-L., and Schleiss, A. J.: Hydropeaking indicators for characterization of the Upper-Rhone River in Switzerland, Aquatic Sciences, 73, 171–182, doi:10.1007/s00027-010-0154-7, 2010.

Merz, R., Parajka, J., and Blöschl, G.: Time stability of catchment model parameters: Implications for climate impact analyses, Water Resources Research, 47, W02 531, doi:10.1029/2010WR009505, 2011.

Mölg, T., Cullen, N. J., and Kaser, G.: Solar radiation, cloudiness and longwave radiation over low-latitude glaciers: implications for mass-balance modelling, Journal of Glaciology, 55, 292–302, doi:10.3189/002214309788608822, 2009.

Nash, J. and Sutcliffe, J.: River flow forecasting through conceptual models part I – A discussion of principles, Journal of Hydrology, 10, 282–290, doi:10.1016/0022-1694(70)90255-6, 1970.

Naz, B. S., Frans, C. D., Clarke, G. K. C., Burns, P., and Lettenmaier, D. P.: Modeling the effect of glacier recession on streamflow response using a coupled glacio-hydrological model, Hydrol. Earth Syst. Sci., 18, 787–802, doi:10.5194/hess-18-787-2014, 2014.

Ng, F., Liu, S., Mavlyudov, B., and Wang, Y.: Climatic control on the peak discharge of glacier outburst floods, Geophysical Research Letters, 34, L21 503, doi:10.1029/2007GL031426, 2007.

Nicholson, L. and Benn, D. I.: Calculating ice melt beneath a debris layer using meteorological data, Journal of Glaciology, 52, 463–470, doi:10.3189/172756506781828584, 00078, 2006.

Oesterle, H., Gerstengarbe, F., and Werner, P.: Homogenisierung und Aktualisierung des Klimadatensatzes des Climate Research Unit der Universität of East Anglia, Norwich: University of East Anglia, 2003.

Osmonov, A., Bolch, T., Xi, C., Kurban, A., and Guo, W.: Glacier characteristics and changes in the Sary-Jaz River Basin (Central Tien Shan, Kyrgyzstan) – 1990–2010, Remote Sensing Letters, 4, 725–734, doi:10.1080/2150704X.2013.789146, 2013.

Paul, F.: The new Swiss glacier inventory 2000: Application of Remote Sensing and GIS, Ph.D. thesis, Department of Geography, University of Zurich, 2003.

Paul, F.: The influence of changes in glacier extent and surface elevation on modeled mass balance, The Cryosphere, 4, 569–581, doi:10.5194/tc-4-569-2010, 2010.

Peel, M. C. and Blöschl, G.: Hydrological modelling in a changing world, Progress in Physical Geography, 35, 249–261, doi:10.1177/0309133311402550, 2011.

Pellicciotti, F., Buergi, C., Immerzeel, W. W., Konz, M., and Shrestha, A. B.: Challenges and Uncertainties in Hydrological Modeling of Remote Hindu Kush–Karakoram–Himalayan (HKH) Basins: Suggestions for Calibration Strategies, Mountain Research and Development, 32, 39–50, doi:10.1659/MRD-JOURNAL-D-11-00092.1, 2012.

Pieczonka, T. and Bolch, T.: Region-wide glacier mass budgets and area changes for the Central Tien Shan between ~ 1975 and 1999 using Hexagon KH-9 imagery, Global and Planetary Change, 128, 1–13, doi:10.1016/j.gloplacha.2014.11.014, 2015.

Quick, M. C. and Pipes, A.: U.B.C. WATERSHED MODEL / Le modèle du bassin versant U.C.B, Hydrological Sciences Bulletin, 22, 153–161, doi:10.1080/02626667709491701, 1977.

Rahman, K., Maringanti, C., Beniston, M., Widmer, F., Abbaspour, K., and Lehmann, A.: Streamflow Modeling in a Highly Managed Mountainous Glacier Watershed Using SWAT: The Upper Rhone River Watershed Case in Switzerland, Water Resources Management, 27, 323–339, doi:10.1007/s11269-012-0188-9, 2012.

Rasemann, S., Schmidt, J., Schrott, L., and Dikau, R.: Geomorphometry in Mountain Terrain, in: Geographic Information Science and Mountain Geomorphology, pp. 101–137, Springer Science & Business Media, 2004.

Refsgaard, J. C.: Parameterisation, calibration and validation of distributed hydrological models, Journal of Hydrology, 198, 69–97, doi:10.1016/S0022-1694(96)03329-X, 1997.

Rowan, A. V., Egholm, D. L., Quincey, D. J., and Glasser, N. F.: Modelling the feedbacks between mass balance, ice flow and debris transport to predict the response to climate change of debris-covered glaciers in the Himalaya, Earth and Planetary Science Letters, 430, 427–438, doi:10.1016/j.epsl.2015.09.004, 2015.

Sakai, A., Nakawo, M., and Fujita, K.: Melt rate of ice cliffs on the Lirung Glacier, Nepal Himalayas, 1996, Bulletin of glacier research, pp. 57–66, 1998.

Sakai, A., Takeuchi, N., Fujita, K., and Nakawo, M.: Role of supraglacial ponds in the ablation process of a debris-covered glacier in the Nepal Himalayas, IAHS-AISH publication, pp. 119–130, 2000.

Schaefli, B.: Quantification of modelling uncertainties in climate change impact studies on water resources: application to a glacier-fed hydropower production system in the Swiss Alps, Ph.D. thesis, École polytechnique fédérale de Lausanne, Lausanne, 2005.

Scherler, D., Bookhagen, B., and Strecker, M. R.: Spatially variable response of Himalayan glaciers to climate change affected by debris cover, Nature Geoscience, 4, 156–159, doi:10.1038/ngeo1068, 2011.

Schweizer, J., Bruce Jamieson, J., and Schneebeli, M.: Snow avalanche formation, Reviews of Geophysics, 41, 1016, doi:10.1029/2002RG000123, 2003.

Sevruk, B.: Systematischer Niederschlagsmessfehler in der Schweiz, Beiträge zur Geologie der Schweiz–Hydrologie, 31, 65–75, 1985.

Sevruk, B. and Mieglitz, K.: The effect of topography, season and weather situation on daily precipitation gradients in 60 Swiss valleys, Water Science and Technology, 00016, 2002.

Shangguan, D. H., Bolch, T., Ding, Y. J., Kröhnert, M., Pieczonka, T., Wetzel, H. U., and Liu, S. Y.: Mass changes of Southern and Northern Inylchek Glacier, Central Tian Shan, Kyrgyzstan, during ∼1975 and 2007 derived from remote sensing data, The Cryosphere, 9, 703–717, doi:10.5194/tc-9-703-2015, 2015.

Sorg, A., Bolch, T., Stoffel, M., Solomina, O., and Beniston, M.: Climate change impacts on glaciers and runoff in Tien Shan (Central Asia), Nature Climate Change, 2, 725–731, doi:10.1038/nclimate1592, print October 2012.

Stisen, S., Højberg, A. L., Troldborg, L., Refsgaard, J. C., Christensen, B. S. B., Olsen, M., and Henriksen, H. J.: On the importance of appropriate precipitation gauge catch correction for hydrological modelling at mid to high latitudes, Hydrol. Earth Syst. Sci., 16, 4157–4176, doi:10.5194/hess-16-4157-2012, 00014, 2012.

Taylor, K. E., Stouffer, R. J., and Meehl, G. A.: An Overview of CMIP5 and the Experiment Design, Bulletin of the American Meteorological Society, 93, 485–498, doi:10.1175/BAMS-D-11-00094.1, 2011.

Uhlmann, B., Jordan, F., and Beniston, M.: Modelling runoff in a Swiss glacierized catchment—part I: methodology and application in the Findelen basin under a long-lasting stable climate, International Journal of Climatology, 33, 1293–1300, doi:10.1002/joc.3501, 2013.

Vieli, A.: Glacier change: Dynamic projections, Nature Geoscience, 8, 332–333, doi:10.1038/ngeo2425, 2015.

Weedon, G. P., Gomes, S., Viterbo, P., Shuttleworth, W. J., Blyth, E., Oesterle, H., Adam, J. C., Bellouin, N., Boucher, O., and Best, M.: Creation of the WATCH Forcing Data and Its Use to Assess Global and Regional Reference Crop Evaporation over Land during the Twentieth Century, Journal of Hydrometeorology, 12, 823–848, doi:10.1175/2011JHM1369.1, 00081, 2011.

WGMS and UNEP: Global glacier changes: facts and figures, World Glacier Monitoring Service, Zürich, 2008.

Winsemius, H. C., Schaefli, B., Montanari, A., and Savenije, H. H. G.: On the calibration of hydrological models in ungauged basins: A framework for integrating hard and soft hydrological information, Water Resources Research, 45, W12 422, doi:10.1029/2009WR007706, 2009.

Wortmann, M., Krysanova, V., Kundzewicz, Z. W., Su, B., and Li, X.: Assessing the influence of the Merzbacher Lake outburst floods on discharge using the hydrological model SWIM in the Aksu headwaters, Kyrgyzstan/NW China, Hydrological Processes, 28, 6337–6350, doi:10.1002/hyp.10118, 2014.

Yatagai, A., Kamiguchi, K., Arakawa, O., Hamada, A., Yasutomi, N., and Kitoh, A.: APHRODITE: Constructing a Long-Term Daily Gridded Precipitation Dataset for Asia Based on a Dense Network of Rain Gauges, Bulletin of the American Meteorological Society, 93, 1401–1415, doi:10.1175/BAMS-D-11-00122.1, 00128, 2012.

Zemp, M., Hoelzle, M., and Haeberli, W.: Six decades of glacier mass-balance observations: a review of the worldwide monitoring network, Annals of Glaciology, 50, 101–111, doi:10.3189/172756409787769591, 2009.

Zhang, Y., Liu, S., and Ding, Y.: Observed degree-day factors and their spatial variation on glaciers in western China, Annals of Glaciology, 43, 301–306, doi:10.3189/172756406781811952, 00037, 2006.

Hydrol. Earth Syst. Sci. Discuss., doi:10.5194/hess-2016-272, 2016
Manuscript under review for journal Hydrol. Earth Syst. Sci.
Published: 16 June 2016

Hydrology and Earth System Sciences
Open Access
Discussions

Table 1. Calibration parameters ordered by model component with typical ranges.

Parameter	Description	Range	Unit
Snow and glaciers			
δ_s	Snow Degree-Day factor	2 – 4	mm °C^{-1} d^{-1}
T_s T_m	Snow fall and melt threshold temperatures	0 ± 2	°C
t_e	Temperature lapse rate	-0.45 – -0.70	°C/100m
δ_g	Ice Degree-Day factor	7.5 – 10	mm °C^{-1} d^{-1}
b_r	Residual mass balance during initialisation	0 ± 300	mm a^{-1}
*Precipitation**			
c	Maximum correction factor	1–10	
a	Maximum precipitation gradient	0.05 – 0.4	% m^{-1}
m	Maximum precipitation altitude	3000–7000	m asl.
Hydrology			
E_c	evaporation correction	0.95 – 1.5	
R_2 R_4	routing coefficients	1 – 5	
S_c	saturated conductivity correction	0.5 – 2	

*only used for the data-scarce Aksu catchment

Table 2. Catchment details according to the gauging stations used for calibration; drainage area, mean discharge Q as annual mean and summer mean for the month June to August (over all available data) and glacier cover. See Tab. Table 3 for sources.

Gauge station	River	Area $[km^2]$	mean Q $[m^3s^{-1}]$	mean JJA Q $[m^3s^{-1}]$	Glacier [%]
Upper Aksu					
Xiehela	Kumarik R.	12991	151.8	406.6	22
Sary-Djaz	Sary-Djaz R.	1927	37.4	91.3	18
Upper Rhone					
Port du Scex	Rhone R.	5220	180.3	349.5	11.9
Blatten	Massa R.	192	2.8	7.6	57

Hydrol. Earth Syst. Sci. Discuss., doi:10.5194/hess-2016-272, 2016
Manuscript under review for journal Hydrol. Earth Syst. Sci.
Published: 16 June 2016

Hydrology and Earth System Sciences
Open Access
Discussions

Table 3. Input data used to drive SWIM and to calibrate/validate the model. Topography and glaciers are shown in Fig. Figure 3. Climate variables are: temperature T (mean, min., max.), precipitation P, radiation and relative humidity.

Data	Upper Aksu	Upper Rhone
Climate	WATCH (Weedon et al., 2011) for T, radiation and relative humidity; P from APHRODITE (Yatagai et al., 2012)	climate reference data from Oesterle et al. (2003) with additional precipitation observations from MeteoSwiss
Topography	SRTM digital elevation model at 90m (hole-filled) (Jarvis et al., 2007)	ASTER digital elevation model at 30m (GDEMv2, hole-filled)
Land cover	Chinese Meteorological Administration for Chinese part, MODIS 500 m land cover (2001) (Friedl et al., 2002) for Kyrghyz part	CORINE Land Cover (European Environment Agency, 2006)
Glaciers	Outlines for 1975 by Pieczonka and Bolch (2015); Osmonov et al. (2013) and simulated volume (Duethmann et al., 2015)	Outlines for 1973 by Paul (2003) and simulated volumes by Linsbauer et al. (2012).
Soil	Harmonised World Soil Database (FAO, 2011)	
Discharge	Xiehela station from Chinese hydrological yearbooks and Sary-Djaz station from Kirghiz hydrological yearbooks.	Port du Scex and Blatten from GRDC (2016)

Hydrol. Earth Syst. Sci. Discuss., doi:10.5194/hess-2016-272, 2016
Manuscript under review for journal Hydrol. Earth Syst. Sci.
Published: 16 June 2016

Hydrology and Earth System Sciences
Open Access
Discussions

Table 4. Model performance for all four objectives: median (min., max.). The Nash-Sutcliff Efficiency **NSE** and the bias in the water balance **PB** are given for the calibration and validation period (split-sample approach). The absolute and relative error of the glacier area hypsometry **A** is given as a fraction of total glacier area. The simulated annual mass balances **MB** are compared to observed values by Pieczonka and Bolch (2015) (Upper Aksu) and Fischer et al. (2015) (Upper Rhone).

Station	**NSE** *calibration* *validation*	**PB** [%] *calibration* *validation*	**A** [%] *abs. residuals* *rel. total*	**MB** [m w.e. a^{-1}] *simulated* *observed*
Upper Aksu				
Xiehela	0.82 (0.81, 0.83)	0.8 (-4.4, 2.3)	16.3 (14.2, 19.5)	-0.36 (-0.37, -0.34)
	0.84 (0.82, 0.85)	-2.4 (-7.7, -1.1)	-1.1 (-11.5,2.4)	-0.35 ± 0.34
Sary-D.	0.63 (0.60, 0.70)	0.8 (-2.6, 5.3)	25.9 (18.7, 31.2)	-0.33 (-0.37, -0.33)
	0.66 (0.61, 0.72)	-7.9 (-11, -3.7)	11.3 (-5.3,18.5)	-0.35 ± 0.34
Upper Rhone				
Port d. S.	0.67 (0.66, 0.68)	-1.8 (-2.8, -1.4)	12.6 (10.8, 15.8)	-0.67 (-0.72, -0.58)
	0.62 (0.60, 0.64)	0.8 (-0.3, 1.4)	-8.8 (-13.8,6.8)	-0.59 ± 0.07
Blatten	0.89 (0.86, 0.90)	-0.1 (-1.0, 1.0)	8.4 (7.2, 10.0)	-0.87 (-0.96, -0.80)
	0.89 (0.85, 0.90)	-2.7 (-4.7, 0.6)	-1.0 (-6.7,2.1)	-0.80 ± 0.07

Hydrology and Earth System Sciences
Open Access
Discussions

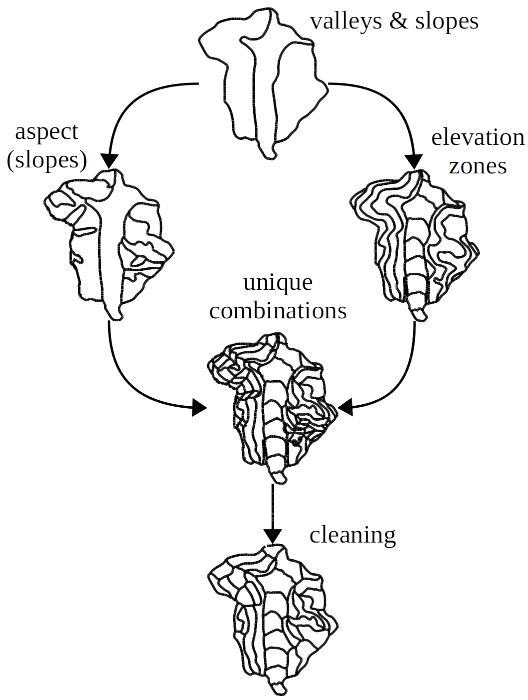

Figure 1. Spatial disaggregation within a subbasin as the representative glacier units.

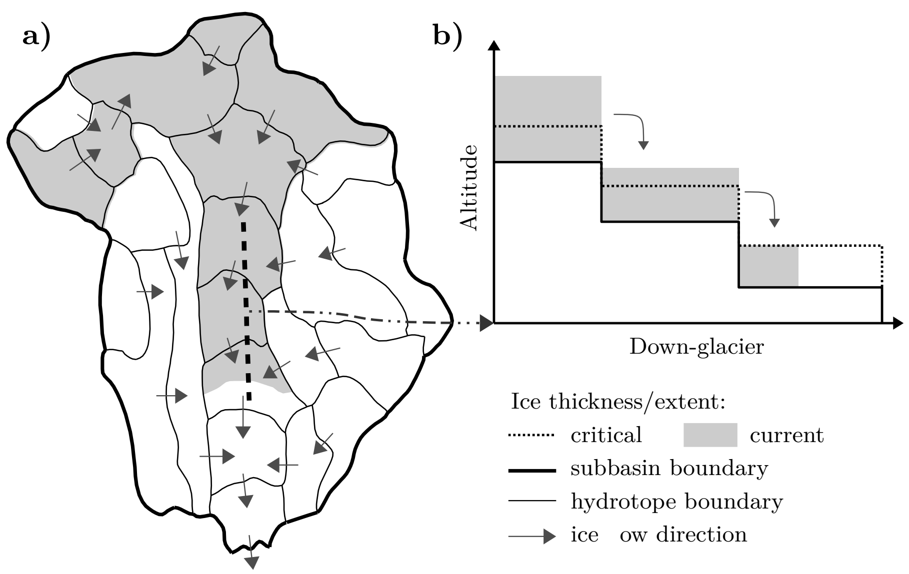

Figure 2. Schematic representation of ice routing in a single subbasin (a) and through a valley cross-section of three glacier units (b).

Hydrol. Earth Syst. Sci. Discuss., doi:10.5194/hess-2016-272, 2016
Manuscript under review for journal Hydrol. Earth Syst. Sci.
Published: 16 June 2016

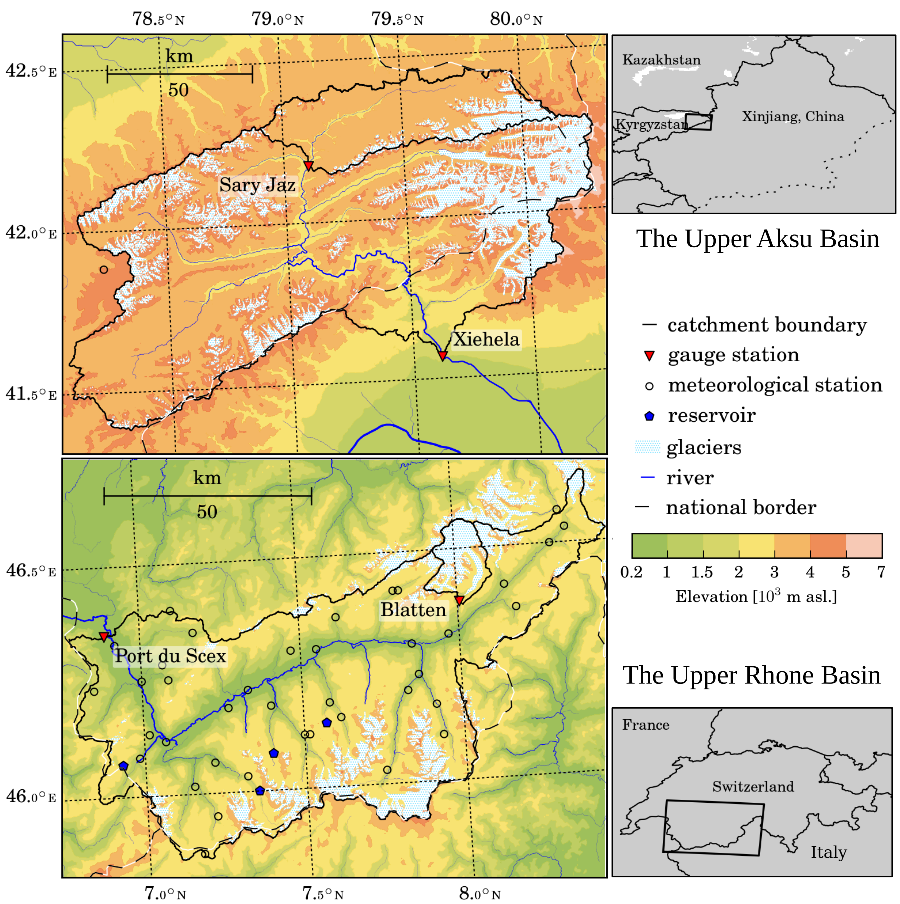

Figure 3. Overview maps of the two case study basins. Glacier cover is only shown inside the catchments.

Hydrol. Earth Syst. Sci. Discuss., doi:10.5194/hess-2016-272, 2016
Manuscript under review for journal Hydrol. Earth Syst. Sci.
Published: 16 June 2016

Hydrology and Earth System Sciences
Discussions

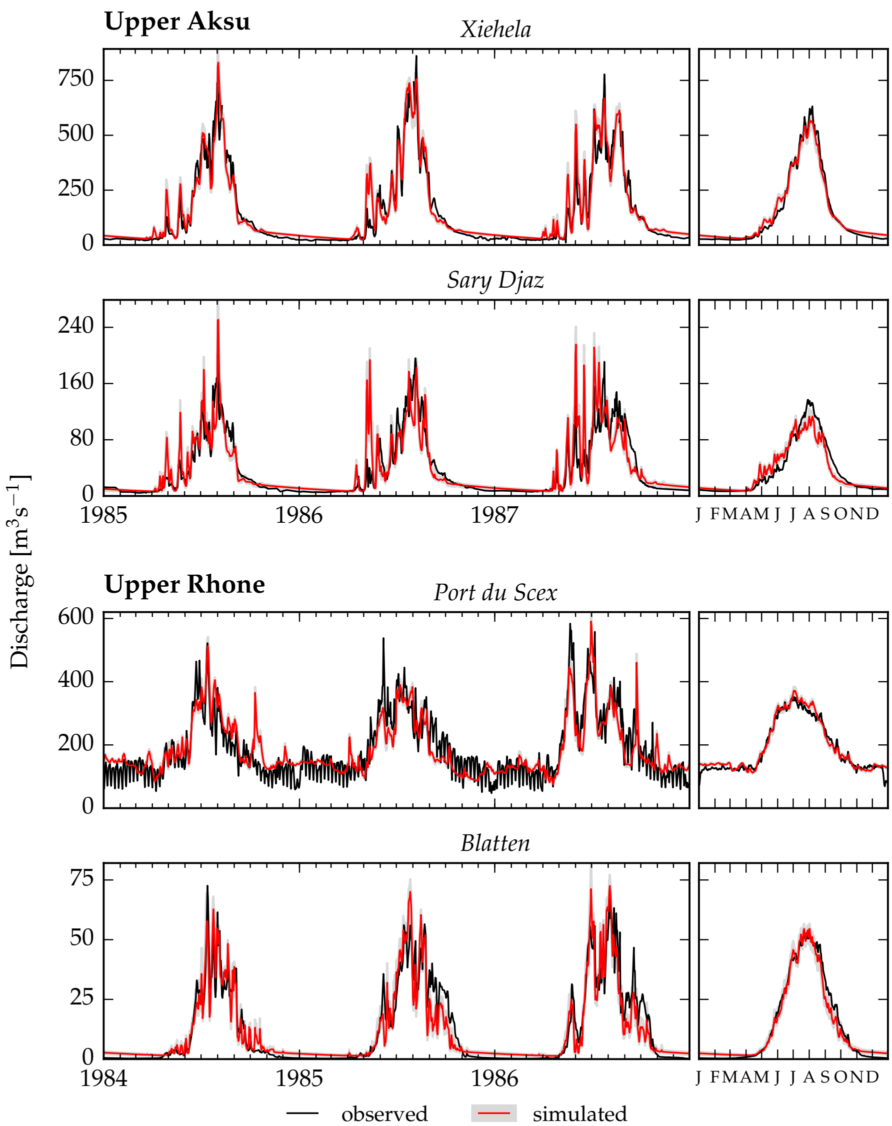

Figure 4. Calibrated discharge for the outlet stations (Xiehela and Port du Scex) and intermediate stations (Sarj Djaz and Blatten) of both catchments. Daily discharge (left) is shown for a selected period while day of year mean discharge (right) is taken over the entire calibration and validation period.

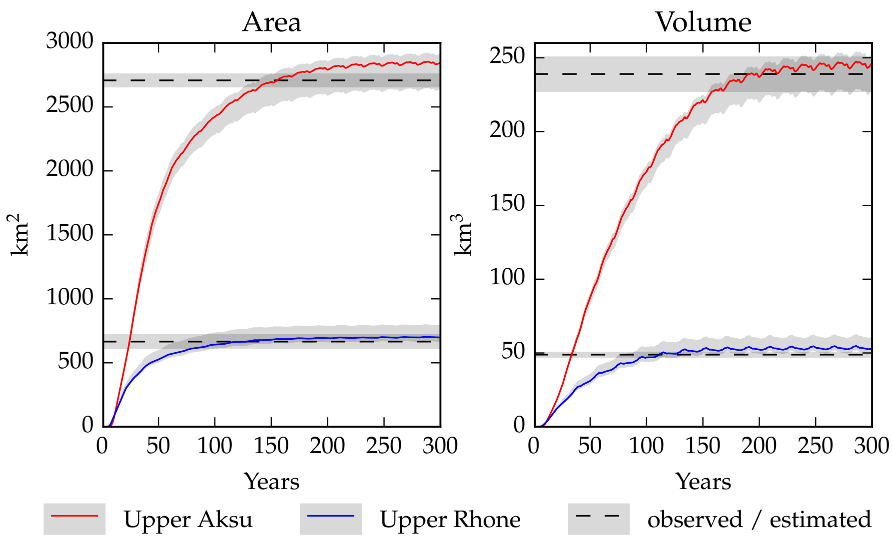

Figure 5. Development of area and volume over the 300-year initialisation period in the Upper Rhone and the much larger Upper Aksu catchment. Observed area ranges are taken from Paul (2003) and Pieczonka and Bolch (2015); Osmonov et al. (2013). Volume estimations are based on modelled glacier thicknesses in the Upper Aksu catchment and in the Upper Rhone catchment by Linsbauer et al. (2012).

Hydrol. Earth Syst. Sci. Discuss., doi:10.5194/hess-2016-272, 2016
Manuscript under review for journal Hydrol. Earth Syst. Sci.
Published: 16 June 2016

Hydrology and Earth System Sciences
Discussions

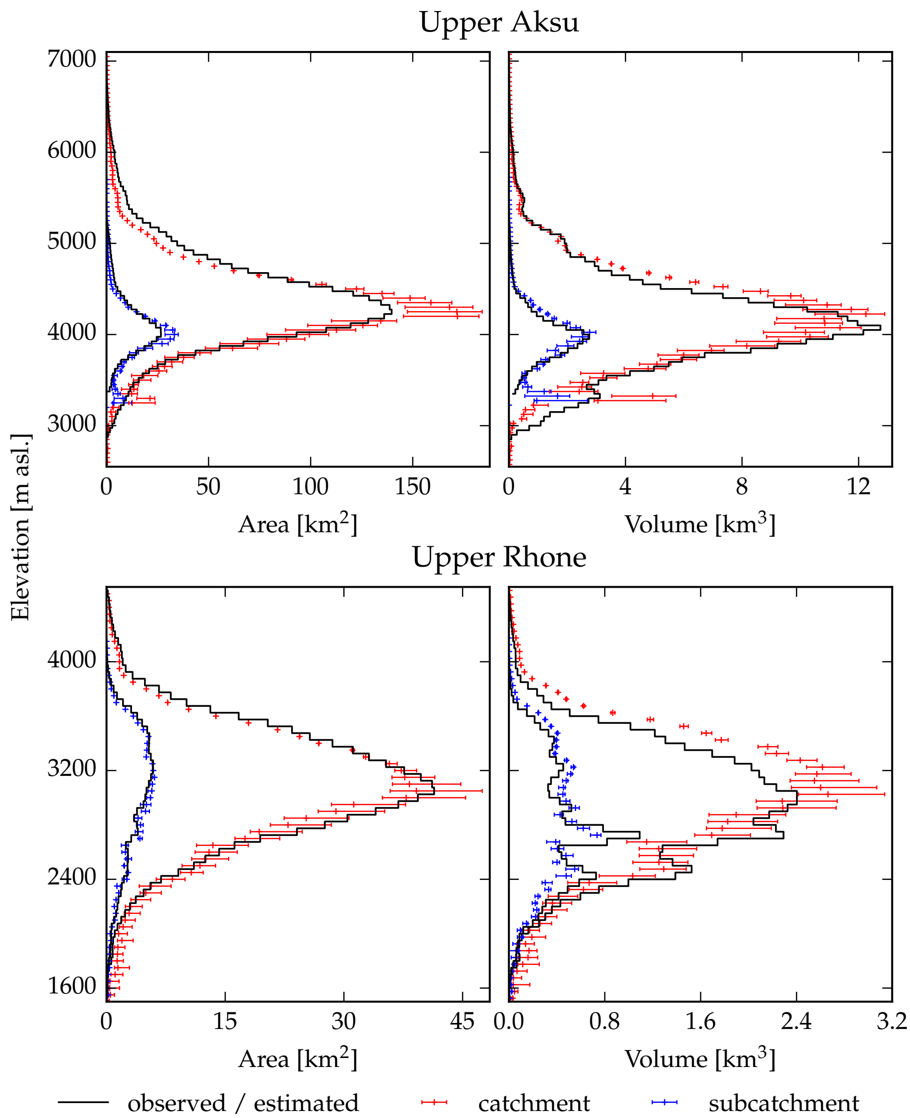

Figure 6. Initialised glacier area and volume hypsometry (i.e. distribution over 50m elevation zones). The catchment-wide hypsometry is shown with the subcatchments of the Sary-Djaz gauge station in the Upper Aksu catchment and the Blatten station in the Rhone catchment, which encompasses the Great Aletsch Glacier. Observed areas are taken from Pieczonka and Bolch (2015) in the Upper Aksu catchment and from Paul (2003). Volume estimations are based on modelled glacier thicknesses in the Upper Aksu catchment by Pieczonka and Bolch (2015) and in the Upper Rhone catchment by Linsbauer et al. (2012).

Hydrology and Earth System Sciences
Open Access
Discussions

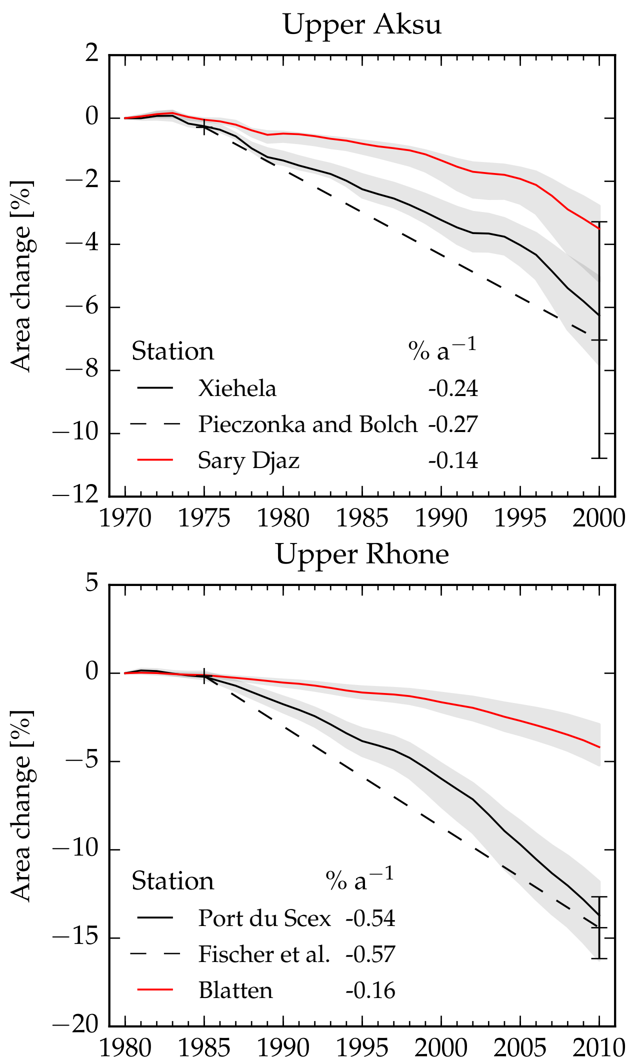

Figure 7. Median of simulated relative glacier area changes including ranges induced by the parameter uncertainty. The observed geodetic area changes from the indicated studies are shown by the dashed line with uncertainty ranges. Mean values over the simulation period are indicated in the legend.

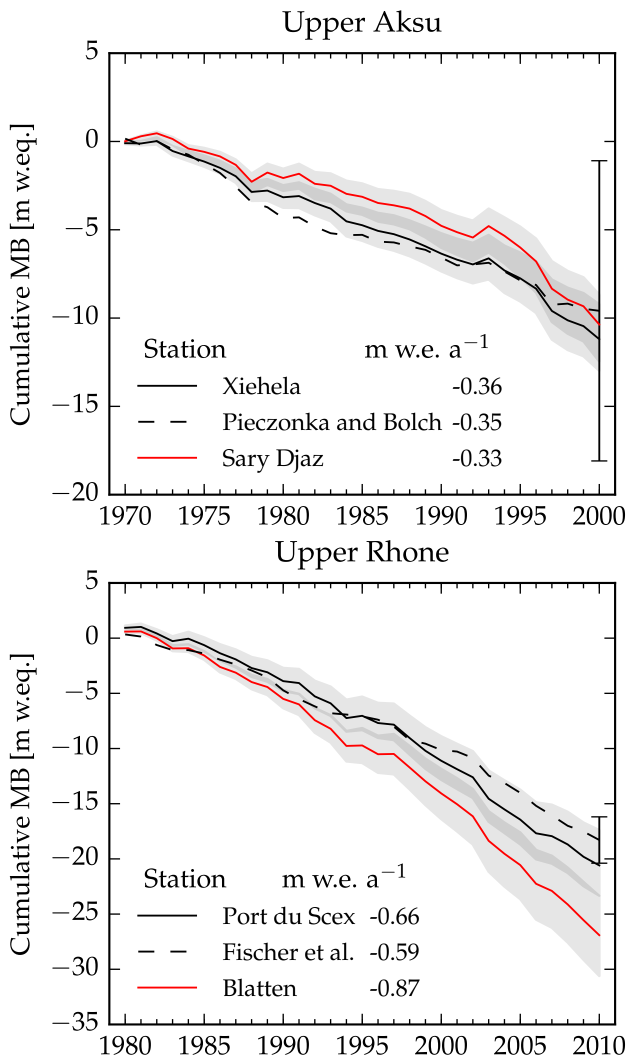

Figure 8. Median of simulated mass changes including ranges induced by the parameter uncertainty. The dashed black line shows the reference glacier mass balance scaled by the catchment-wide geodetic mass balance from the indicated studies including uncertainty bars from those studies. Note that the scaled/observed mass balance and the uncertainty bar (black) only refers to the entire catchment, i.e. the outlet station. Annual mean values over the simulation period are indicated in the legend.

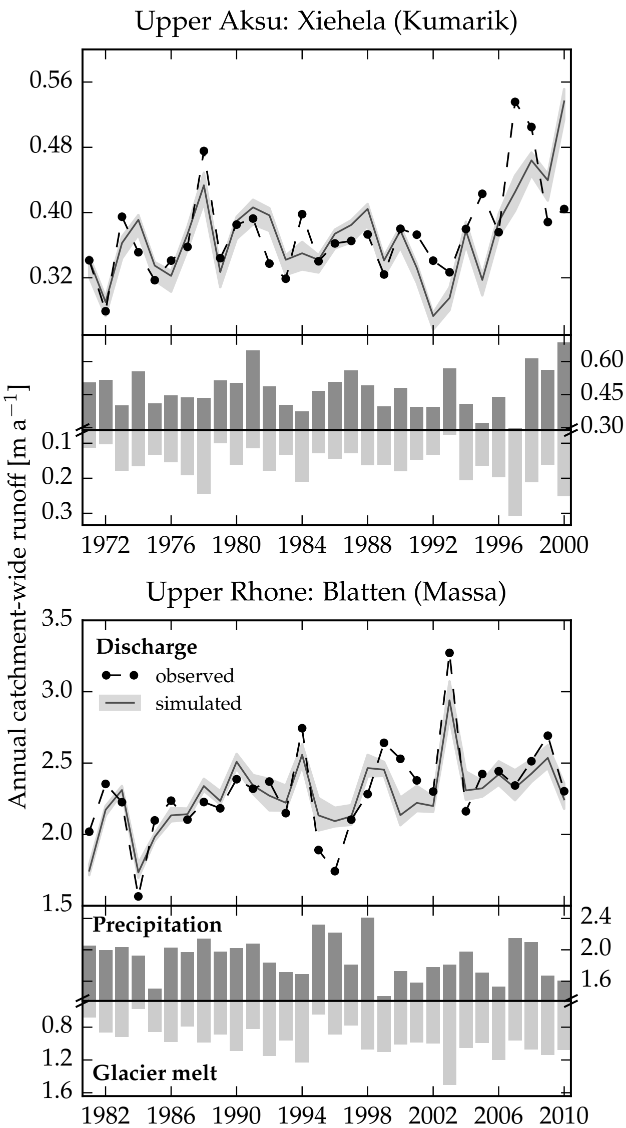

Figure 9. Simulated (median, min., max.) and observed mean annual discharge at Xiehela (Kumarik) and Blatter (Massa) stations with annual precipitation and glacier melt distributed over the catchment area.